

Estimating the Hallucination Rate of Generative AI

Andrew Jesson^{*†}Nicolas Beltran-Velez^{*‡}Quentin Chu[‡]Sweta Karlekar[‡]Jannik Kossen[§]Yarin Gal[§]John P. Cunningham[†]David Blei^{†‡}

Abstract

This work is about estimating the hallucination rate for in-context learning (ICL) with generative AI. In ICL, a conditional generative model (CGM) is prompted with a dataset and asked to answer a prediction question based on that dataset. Formally, an ICL problem is a tuple containing a CGM, a dataset, and a prediction question. One interpretation of ICL assumes that the CGM computes the posterior predictive of an unknown Bayesian model. The Bayesian model defines a joint distribution over observable datasets and latent mechanisms, which factorizes into the model likelihood over datasets given a mechanism and the model prior over mechanisms. It is assumed that an ICL dataset comprises independent samples from the model likelihood indexed by a specific mechanism. Moreover, that the prediction question and any valid response are distributed according to the same likelihood. With this perspective, we define a *hallucination* as a generated response to the prediction question that has low-probability under the model likelihood indexed by the mechanism. We develop a new method that takes an ICL problem and estimates the probability that a CGM will generate a hallucination. Our method only requires generating prediction questions and responses from the CGM and evaluating its response log probability. We empirically evaluate our method on synthetic regression and natural language ICL tasks using large language models.

1 Introduction

This work is about estimating the hallucination rate for in-context learning (ICL). In ICL, we feed a dataset to a conditional generative model (CGM) and ask it to make a prediction based on that dataset [1, 2]. This practice is useful because it allows us to use pre-trained models to solve problems that they may not have been explicitly optimized for. For example, ICL can improve the prediction accuracy of large language models (LLMs) for benchmark tasks in math, translation, and time series prediction [3, 4]. However, it is difficult to understand the errors a particular ICL application might make—in the terminology of Generative AI, such errors are poetically called *hallucinations* [5].

We develop a new method that takes an ICL problem—that is, a CGM, a dataset, and a prediction question—and estimates the probability that it will generate a hallucination in response. Figure 1a shows an ICL problem with news snippets classified as World, Sports, Business, or Science [6], where the last snippet’s correct answer is Sports. Figure 1b displays responses generated by Llama-2-7B, with 25% incorrect.

The main idea is to take a Bayesian perspective of ICL, whereby we assume that the CGM generates samples from the posterior predictive distribution of an (unknown) Bayesian model that defines a joint distribution over observable data and latent mechanisms [7, 8]. We can then define the

^{*}Denotes equal contribution. Correspondence to {adj2147, nb2838}@columbia.edu. [†] Department of Statistics, Columbia University. [‡] Department of Computer Science, Columbia University. [§] OATML, Department of Computer Science, University of Oxford.

Input: This week's schedule TODAY'S GAMES Division 1 GREATER BOSTON --Arlington at Malden...
Label: Sports
Input: Putting Nature on the Pill Wildlife managers are looking to contraception as a way...
Label: Science
Input: Error of Judgment The FBI alleges that a veteran U.S. diplomat met with agents from...
Label: World
Input: Sears and Kmart to Merge After much speculation, two discount giants move to create...
Label: Business
Input: Defeat for GB canoeists British canoeists Nick Smith and Stuart Bowman are out of...
Label:

(a) An in-context learning dataset.

Sports, Olympics, Other, Sports, Sports, Sports, Sports, Sports, Sports, Sports, Sports,
Athletics, Sports, Entertainment, Sports, Sports, Sports, Sports, Olympics, Sports, Sports,
Olympics, Sports, Sports

(b) Generated responses

Figure 1: An example of an in-context dataset and generated response examples for the last label. The correct response, "Sports", is given in green and wrong answers are given in purple.

posterior hallucination rate (PHR) under this model, which conditions on the observed data (here, the "context"). Finally, we show how to estimate the posterior hallucination rate using the predictive distribution of a CGM.

Related work. Hallucination prediction and mitigation is an active area of research [9–30]. This work is most closely related to a subset of methods based on uncertainty quantification [31–38]. Particularly those methods that aim to predict hallucinations based on uncertainty about the *meaning* of generated responses [33, 34, 36]. Unlike the latter methods, the PHR does not require external information from auxiliary classifiers and is applicable beyond language tasks. Our approach is enabled by sampling ICL dataset completions from the predictive distribution, which was first explored in the context of sequential models by Fong et al. [39]. Extensions to various CGMs are an active area of research [40, 41]. Notably, Falck et al. [41] studies the hypothesis that ICL performs Bayesian inference. It proposes a method, which is similar to ours, to test that hypothesis, and it presents several ICL problems where the hypothesis does not hold.

Contributions. In Section 2, we introduce the *posterior hallucination rate* for Bayesian CGMs, prove that it can be computed by sampling from the predictive distribution, and provide a finite-sample estimator for CGMs that only further requires evaluating the log probabilities of responses. In Section 3, we empirically evaluate our methods. We study the PHR estimator with synthetic data to demonstrate that it can accurately predict the true hallucination rate. We then study our methods on natural language ICL problems with pre-trained CGMs from the Llama-2 [42] and Gemma-2 [43] model families. We demonstrate that the PHR estimator gives accurate estimates of the empirical error rate.

2 The posterior hallucination rate and how to estimate it

In this section, we review the basics of conditional generative models (CGMs). We define in-context learning (ICL) and discuss the Bayesian perspective. We define hallucinations and hallucination rates. Finally, we show how to estimate the hallucination rate given an ICL problem and a CGM.

Conditional generative models and in-context learning. A *conditional generative model* (CGM) is a sequential model of the form $p_{\theta}(t \mid (t_i)_1^n)$ where θ represents the parameters of the model and t_i represents the elements over which the distribution is defined. If the support of each conditional distribution is over language tokens and the size of θ is large, these models are known as large language models (LLMs). We focus on LLMs, but our methods are applicable to many conditional generative models.

Conditional generative models over sequences are most commonly implemented through sequential neural network architectures called Transformers [44]. The parameters θ are set by performing stochastic maximization of the model likelihood over a training dataset $\mathcal{D} = \{(t_i^j)_1^n\}_{j=1}^m$, where i is the index over elements of a sequence and j is the index over sequences. The resulting generative model approximates the distribution of sequences of data in the training dataset \mathcal{D} .

An *in-context learning* (ICL) problem is a tuple $(p_\theta, \mathcal{D}_n, x)$ containing a model p_θ , a dataset \mathcal{D}_n , and a query x . The dataset, or "context", is a sequence of n examples, $\mathcal{D}_n = (x_i, y_i)_{i=1}^n = ((x_1, y_1), \dots, (x_n, y_n))$. For a new query, x , the model is prompted with the query x and context $(x_i, y_i)_{i=1}^n$ to generate a response according to $p_\theta(y \mid (x_i, y_i)_{i=1}^n, x)$.

ICL and Bayesian inference. One way to interpret ICL is from the perspective of Bayesian statistics [7, 8, 45]. In this framework, each individual ICL problem is associated with a *latent mechanism* f^* that defines the task and that governs the data generation process. Given f^* , the data points (x_i, y_i) are drawn independently from the distribution $p_{\text{ICL}}(x_i, y_i \mid f^*)$ ².

Under this assumption, when considering all ICL problems simultaneously, the joint distribution of all query-response pairs can be expressed as a mixture of latent mechanisms f :

$$p_{\text{ICL}}(\mathcal{D}_n) = \int \prod_{i=1}^n p_{\text{ICL}}(x_i, y_i \mid f) dP_{\text{ICL}}(f), \quad (1)$$

If we then further assume that a pre-trained language model p_θ approximates the posterior predictive distribution under this distribution p_{ICL} :

$$p_\theta(y_{n+1} \mid x_{n+1}, \mathcal{D}_n) \approx p_{\text{ICL}}(y_{n+1} \mid x_{n+1}, \mathcal{D}_n) \quad (2)$$

$$= \int p_{\text{ICL}}(y_{n+1} \mid x_{n+1}, f) dP_{\text{ICL}}(f \mid \mathcal{D}_n). \quad (3)$$

then doing ICL using an LLM can be seen as a form of implicit Bayesian inference over the latent mechanisms f [8].

Although Equation (1) can be justified by the definition of an ICL problem or de Finetti-style arguments based on exchangeability [46], Equation (2) must be assumed.

In this paper we show how adopting this approach will allow us to construct and estimate the *posterior hallucination rate*: the probability that a generated response y from p_θ to a query x will be in an unlikely region according to the "true" latent mechanism f^* .

Before we continue, a comment on notation. We use F, X, Y whenever we wish to emphasize that we are referring to random variables, and f, x, y otherwise. For clarity, we use p_θ when referring to the distribution of the CGM and p without a subscript when referring to the probability of the "true" generating process. This could be p_{ICL} or any other probability distribution that follows Equation (1).

2.1 Hallucinations and the posterior hallucination rate

Using the ideas of CGMs and ICL, we now define hallucinations and the hallucination rate.

First, imagine a setting where we observe a true mechanism f^* . For a query x , what values of y would we consider hallucinations? A simple idea is to call hallucinations those values of y that are unlikely to be generated from $p(y \mid x, f^*)$. This motivates the following two definitions.

Definition 1. We define a $(1-\epsilon)$ -likely set of f and x as any set A such that $P(Y \in A \mid f, x) \geq 1 - \epsilon$.

Definition 2. For fixed $(1-\epsilon)$ -likely sets $A(f, x)$, we call a value y a hallucination with respect to x and f , if $y \notin A(x, f)$.

As a simple intuitive example, assume that the true generative model of $(x_i, y_i)_{i=1}^n$ is a Bayesian linear model with a known standard deviation σ . Specifically, $f \sim \mathcal{N}(0, I_d)$, $x_i \sim \mathcal{N}(0, I_d)$, and $y_i \sim \mathcal{N}(f^\top x_i, \sigma^2)$, where $f, x_i \in \mathbb{R}^d$ and $y_i \in \mathbb{R}$. If $\epsilon = 0.05$, we could choose the interval between the 2.5 and 97.5 percentiles of the distribution $\mathcal{N}(f^{*\top} x, \sigma^2)$ as our $(1-\epsilon)$ -likely set and call everything outside of this interval a hallucination.

In practice, we do not observe f^* . Rather, we make predictions with $p(y \mid x, \mathcal{D}_n)$. We ask: At what rate are we hallucinating when we make predictions? The answer is the *true hallucination rate*.

² When there is a finite number of possible (x, y) pairs, such as in large language models (LLMs), each f can be represented as a large vector. Each element of this vector corresponds to a specific (x, y) pair, and $f_{x,y}$ represents the probability $P(X = x, Y = y)$, as described in [45]. In other words, f is simply the probability distribution. In turn, given a finite support and the conditional independence of pairs given the task, we can assume the existence of the latent mechanism f^* by identifying it directly with $P(X = x, Y = y)$ for each task.

Definition 3. We define the true hallucination rate (THR) as the probability of sampling a hallucination given true mechanism f^* and query x :

$$h_\epsilon^*(f^*, x) := \int \mathbb{1}\{y \notin A(f^*, x)\} dP(y \mid \mathcal{D}_n, x). \quad (4)$$

Where $A(f^*, x)$ is an $(1 - \epsilon)$ -likely set of f^* and x .

This value is higher when the posterior predictive $p(y \mid \mathcal{D}_n, x)$ places high probability in regions unlikely under $p(y \mid f^*, x)$, or very low if the posterior predictive puts a lot of mass on areas likely under $p(y \mid f^*, x)$. We expect the value to be higher when we don't have enough examples and lower as the dataset size increases.

Of course, we do not observe the true mechanism f^* . But the dataset ("context") \mathcal{D}_n provides evidence for it, as summarized in the posterior $p(f \mid \mathcal{D}_n)$. With this distribution we define the *posterior hallucination rate*, which is the centerpiece of this work.

Definition 4. We define the posterior hallucination rate (PHR) as

$$h_\epsilon(x) := \mathbb{E}[h_\epsilon^*(F, x) \mid \mathcal{D}_n] = \iint \mathbb{1}\{y \notin A(f, x)\} dP(y \mid \mathcal{D}_n, x) dP(f \mid \mathcal{D}_n). \quad (5)$$

In linear regression, the PHR is the probability that y will land outside of the high probability interval of f and x when sampling $F \sim p(f \mid \mathcal{D}_n)$, the posterior over coefficients, and $Y \sim p(y \mid \mathcal{D}_n, x)$, the posterior predictive over responses.

Here we remind the reader that we still cannot calculate $p(f \mid \mathcal{D}_n)$ from the CGM. But we will address this problem in the next section.

As a final detail, we discuss how to construct $(1-\epsilon)$ -likely sets. Ideally, we would like these sets to be constructed so that we can check if $y \in A(f, x)$ easily. Otherwise, it would be hard to know if a response y is a hallucination. One way to do so is to define a statistic S that maps each value in \mathcal{Y} to a value in \mathbb{R} . We then define $Q_\epsilon(f, x)$ as the ϵ quantile of this statistic under $p(y \mid f, x)$. Because it is a quantile,

$$P(Y \in \{y \mid S(y) \geq Q_\epsilon(f, x)\} \mid f, x) \geq 1 - \epsilon.$$

Thus, $A(f, x) = \{y \mid S(y) \geq Q_\epsilon(f, x)\}$ is an $(1-\epsilon)$ -likely set.

One convenient choice of S is $\log p(y \mid x, f)$. Thus, moving forward, we let

$$A(f, x) = \{y : \log p(y \mid x, f) \geq Q_\epsilon(f, x)\} \quad (6)$$

and we replace all statements $\mathbb{1}\{y \notin A(f, x)\}$ with $\mathbb{1}\{\log p(y \mid f, x) < Q_\epsilon(f, x)\}$ in the definitions of a hallucination, the true hallucination rate, and the posterior hallucination rate.

2.2 Calculating the posterior hallucination rate from predictive distributions

Our goal is to calculate the posterior hallucination rate from Definition 4. However, conditional generative models like LLMs only provide an approximation to the predictive distribution $p(x, y \mid \mathcal{D}_n)$ rather than the posterior over mechanisms $p(f \mid \mathcal{D}_n)$ or the response likelihood, $p(y \mid x, f)$. To overcome this limitation, we propose Algorithm 1, which uses a CGM to estimate the PHR.

We will first explain Algorithm 1 intuitively, without appealing to Bayesian statistics and only after we will provide a formal justification of how it returns an estimate of Definition 4.

As input, Algorithm 1 receives an ICL problem, a budget for MC samples M , and a maximum context length to process N . First, it samples $N - n$ new query-response pairs according to the predictive distribution $p_\theta(x_N, y_N, \dots, x_{n+1}, y_{n+1} \mid \mathcal{D}_n)$ (Alg.1, lines 2-6). This can be thought-of as asking the model to imagine future pairs it will receive.

Next, it samples a new response y_{new} from $p(y \mid x, \mathcal{D}_n)$ (Alg.2, line 9) and asks: Is this response likely for x given the task implied by $\mathcal{D} = (x_1, y_1, \dots, x_N, y_N)$ (Alg.1, line 10)? If the model is confident about the task it is performing, the pair (x, y_{new}) will be coherent with $(x_i, y_i)_{n+1}^N$. If the model is uncertain then y_{new} will not be coherent with $(x_i, y_i)_{n+1}^N$. To determine coherence, we check whether y_{new} is in the tails of $\log p_\theta(y_i \mid \mathcal{D}, x)$ (Algorithm 2, Lines 5 and 10).

Algorithm 1 $\widehat{\text{PHR}}(x, \mathcal{D}_n, p_\theta, M, N, K)$

Require: Query x , context $\mathcal{D}_n = (x_i, y_i)_{i=1}^n$, CGM p_θ , number of context samples M , number of THR samples K , max context length N .

```
1: for  $i \leftarrow 1$  to  $M$  do
2:   // Sample imagined context
3:    $\mathcal{D} \leftarrow \mathcal{D}_n$ 
4:   for  $j \leftarrow n+1$  to  $N$  do
5:      $(x_j, y_j) \sim p_\theta(x, y \mid \mathcal{D})$ 
6:      $\mathcal{D} \leftarrow \mathcal{D} \cup (x_j, y_j)$ 
7:   // True hallucination rate
8:    $h_{\epsilon, N, i}^* \leftarrow \widehat{\text{THR}}(x, \mathcal{D}_n, \mathcal{D}, p_\theta, K)$ 
9: return  $\frac{1}{M} \sum_{i=1}^M h_{\epsilon, N, i}^*$ 
```

Algorithm 2 $\widehat{\text{THR}}(x, \mathcal{D}_n, \mathcal{D}, p_\theta, K)$

Require: Query x , extended context \mathcal{D} , original context \mathcal{D}_n , CGM p_θ , number of samples K .

```
1: //Estimate quantiles
2:  $S \leftarrow \{\}$ 
3: for  $i \leftarrow 1$  to  $K$  do
4:    $y_i \sim p_\theta(y \mid x, \mathcal{D})$ 
5:    $S \leftarrow S \cup \{\log p_\theta(y_i \mid x, \mathcal{D})\}$ 
6:  $\widehat{Q} \leftarrow \epsilon$  quantile of  $S$ 
7: // Frequency of hallucinations
8: for  $i \leftarrow 1$  to  $K$  do
9:    $y_i \sim p_\theta(y \mid x, \mathcal{D}_n)$ 
10:   $h_{\epsilon, i} \leftarrow \mathbb{1}\{\log p_\theta(y_i \mid \mathcal{D}, x) < \widehat{Q}\}$ 
11: return  $\frac{1}{K} \sum_{i=1}^K h_{\epsilon, i}$ 
```

Finally, we average over multiple values y_{new} and over multiple samples $(x_i, y_i)_{i=1}^N$. This provides our estimate for the PHR.

Building on this intuition, we now introduce the theoretical justification based on Doob’s theorem [47]. This theorem shows that, as $n \rightarrow \infty$, drawing a value F from $p(f)$ and evaluating $h(F)$ is equivalent to first sampling $(X_i, Y_i)_{i=1}^n$ and then evaluating $\mathbb{E}[h(F) \mid (X_i, Y_i)_{i=1}^n]$. We state this result below.

Theorem 1 (Doob’s Informal). *For $F \in \mathcal{F}$, $(X_i, Y_i) \in \mathcal{X} \times \mathcal{Y}$, if $(F, (X_i, Y_i)_{i=1}^\infty)$ is distributed such that $F \sim p(F)$ and $X_i, Y_i \sim p(x, y \mid f)$ then, under general conditions, the posterior mean of $h(F)$ given $(X_i, Y_i)_{i=1}^\infty$ is almost surely equal to $h(F)$, as the number of samples goes to infinity. That is,*

$$\lim_{n \rightarrow \infty} \mathbb{E}[h(F) \mid (X_i, Y_i)_{i=1}^n] = h(F) \text{ a.s.}$$

This theorem helps us transform statements about $h(f)$ to statements about $\mathbb{E}[h(F) \mid (x_i, y_i)_{i=1}^n]$, which only depends on $(x_i, y_i)_{i=1}^n$. Thus, we can proceed without direct access to $p(f \mid \mathcal{D}_n)$.

With Doob’s theorem established, we now use it to address the problem of estimating the posterior hallucination rate. The next theorem shows how we can compute this rate without needing direct access to $p(f \mid \mathcal{D}_n)$. The proof is provided in Appendix C.

Theorem 2 (PHR via Posterior Predictive). *Assume that the conditions of Theorem 1 hold for F and X, Y , then,*

$$\begin{aligned} h_\epsilon(x) &= \iint \mathbb{1}\{\log p(y \mid x, f) < Q_\epsilon(f, x)\} dP(y \mid \mathcal{D}_n, x) dP(f \mid \mathcal{D}_n) \\ &= \iint \mathbb{1}\left\{\lim_{N \rightarrow \infty} \log p(y \mid (x_i, y_i)_{i=1}^N, x) < Q_\epsilon((x_i, y_i)_{i=1}^\infty, x)\right\} dP(y \mid \mathcal{D}_n, x) dP((x, y)_{n+1}^\infty \mid \mathcal{D}_n), \end{aligned}$$

where $Q_\epsilon((x_i, y_i)_{i=1}^\infty, x)$ is the ϵ -quantile of $\lim_{N \rightarrow \infty} \log p(Y \mid x, (x_i, y_i)_{i=1}^N)$ under the limiting distribution $\lim_{N \rightarrow \infty} p(Y \mid x, (x_i, y_i)_{i=1}^N)$.

Theorem 2 suggests a natural finite approximation to the PHR where we clip all limits in the expression to a sufficiently large N . Using this approximation, the finite version of the true hallucination rate is

$$h_{\epsilon, N}^*((x_i, y_i)_{i=1}^N, x) := \int \mathbb{1}\{\log p(y \mid (x_i, y_i)_{i=1}^N, x) < Q_\epsilon((x_i, y_i)_{i=1}^N, x)\} dP(y \mid \mathcal{D}_n, x) \quad (7)$$

where $Q_\epsilon((x_i, y_i)_{i=1}^N, x)$ is defined analogously to its infinite counterpart, and the finite version of the posterior hallucination rate is

$$h_{\epsilon, N}(x) := \int h_{\epsilon, N}^*((x_i, y_i)_{i=1}^N, x) dP((x_i, y_i)_{i=1}^N \mid \mathcal{D}_n). \quad (8)$$

With $h_{\epsilon, N}(x)$ and $h_{\epsilon, N}^*((x_i, y_i)_{i=1}^N, x)$ we achieve two goals: first, we avoid using any distribution on f , and second, we express all probabilities in terms of finite sequences.

Finally, we derive an estimator for Equation (8) by replacing p with p_θ and by using Monte Carlo to estimate the integrals and quantiles. This is what Algorithm 1 and Algorithm 2 implement: Algorithm 1 estimates Equation (8) and Algorithm 2 estimates Equation (7).

3 Empirical Evaluation

We empirically evaluate the accuracy and applicability of the Posterior Hallucination Rate (PHR) estimator. We first examine whether the PHR estimator accurately predicts the True Hallucination Rate (THR). We design a synthetic regression experiment for which we can calculate the THR. For in-distribution ICL regression tasks, we find the PHR is a reliable predictor of the THR and demonstrate its robustness to the choice of ϵ parameter value. Moreover, we observe that the accuracy of the PHR estimator is higher for smaller ICL dataset sizes n .

We then evaluate the PHR estimator on natural language ICL, using pre-trained large language models (LLMs). Calculating the THR is not feasible, so we investigate two alternative questions: (1) does the PHR estimator accurately predict the model hallucination rate (defined below in Section 3.2), and (2) can the PHR accurately predict the empirical error rate? We find that the PHR estimator reliably predicts the model hallucination rate, regardless of model performance on a given ICL task. Moreover, the estimator remains robust to different ICL dataset sizes and settings of the ϵ parameter. Additionally, the PHR estimator accurately predicts the empirical error rate of generated responses when ϵ is set to values greater than 0.5. Specifically, its accuracy is influenced by the LLM’s performance on the in-context learning task as the number of in-context examples increases. It achieves higher accuracy when the LLM performs better than a random classifier and lower accuracy when it performs roughly equal to random.

3.1 Synthetic regression tasks

We evaluate the PHR in a setting where we know the true mechanism f^* so that we can compare directly it against the true hallucination rate (THR). We implement a CGM trained on sequences of synthetic regression problems and compare the PHR estimates against the THR on new regression tasks.

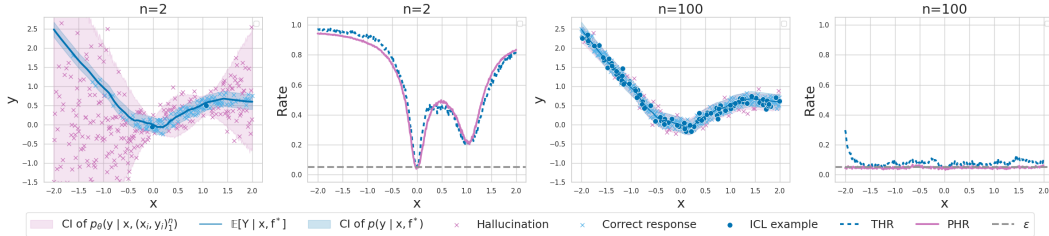


Figure 2: In the first and third panes, we see the neural process’s generated outcomes for $n = 2$ and $n = 100$. The blue region is the true $(1-\epsilon)$ -likely set, while the purple is the likely set when conditioned on the blue data points. The second and fourth panes are the corresponding measures of the PHR and THR across the domain.

Setup. We implement a model with a setup similar to a conditional neural process [48] by modifying the Llama 2 architecture [42] to model sequences of continuous variables. We sample a large set of query-response pairs (x, y) per random re-initialization of the neural network. We define the $(1-\epsilon)$ -likely set with $\epsilon = 0.05$ such that a response y is a hallucination if it falls outside of the 95% confidence interval of a given sampled distribution conditioned on x . Training and test data are generated over non-overlapping sets of generated sequences. Example training datasets are shown in Figure 9a. Example datasets generated by the fit model when initialized with a single random query x are shown in Figure 9b. Full model and dataset details are given in Appendices E.1 and F.1, respectively.

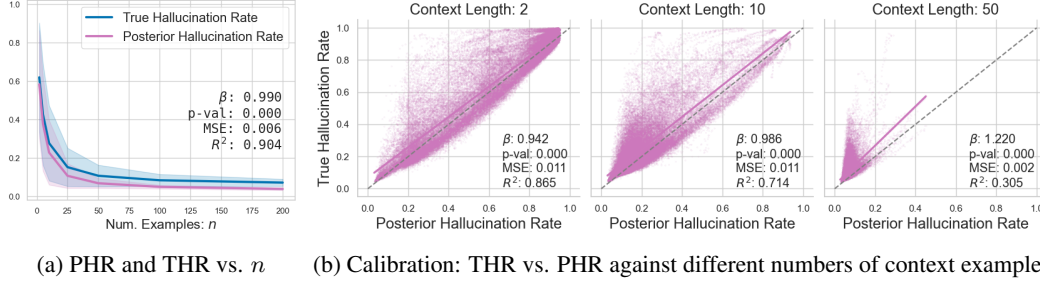


Figure 3: **Synthetic data:** (a) The THR and PHR reduce significantly as the number of contextual examples n increases. (b) Calibration evaluation of the posterior hallucination rate against the true probability of hallucination given $\epsilon = 0.05$.

Results. The first and third panes of Figure 2 show the model’s generated outcomes for $n = 2$ and $n = 100$. The blue region represents the true $(1-\epsilon)$ -likely set for the response distribution of a specific random ReLU neural network. The purple region represents the model’s $(1-\epsilon)$ -likely set when conditioned on the blue data points and a query value x in the domain $[-2, 2]$. As more context examples are provided, confidence intervals shrink, and responses y are more likely to fall within the blue region.

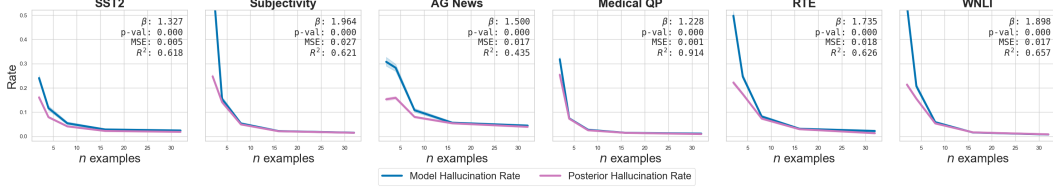
The second and fourth panes of Figure 2 show the true probability of hallucination and PHR for x in the domain $[-2, 2]$ for two settings of n . We set $N - n$ to 100 and M to 40. On the left, dips in PHR and hallucination probability at $x = 0$ and $x = 1$ correspond with the ground truth in-context examples. On the right, with larger n , both PHR and hallucination probability are low across all x values. Notably, PHR and hallucination probability align closely throughout the domain. In Appendix G.1, we show that these findings hold across various settings of the ϵ parameter value.

In Figure 3a, we plot the PHR and true probability of hallucination against increasing context lengths, averaged over 200 random test functions. Although PHR aligns well with THR, it underestimates THR, particularly as the number of examples increases. To understand this better, we examine calibration plots between PHR and THR for different numbers of contextual examples in Figure 3b. For small numbers of contextual examples, PHR closely matches THR, which is encouraging since it is crucial to capture the true probability of hallucination when few examples are present and errors are more likely. These results also support our assumptions about recovering the target estimand through Doob’s Theorem.

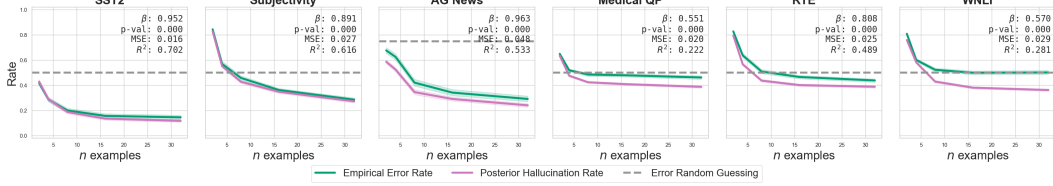
Limitations. To understand the source of the underestimation in the PHR estimator, we consider four potential sources of approximation error. First, the distribution of in-context examples may not be exchangeable due to positional embeddings from the Llama-2 architecture, but this is likely mitigated by training on randomly permuted subsets. Second, Monte-Carlo estimator errors could contribute, but underestimation persists even with increased sample sizes (M or K). Third, the finite number of generated examples ($N - n$) could cause error, but increasing this number beyond 100 shows little bias reduction. Finally, discrepancies between the learned CGM distribution $p_\theta(y | \mathcal{D}_n, x)$ and the true distribution $p(y | \mathcal{D}_n, x)$ can lead to underestimation, as evidenced by differences in confidence intervals around x values of -2 and 1.5 in Figure 2. This discrepancy likely grows with n because accurately modeling $p(y | f^*, x)$ reaches the current limits of in-context learning. Figure 3a shows this discrepancy stabilizes with 200 examples, and Figure 3b shows PHR becomes a less accurate predictor of the true hallucination rate as the number of examples grows. Improving LLM architecture or training procedures could enhance predictive distribution fidelity and PHR estimates as contextual examples increase.

3.2 Natural language tasks

Here we evaluate the posterior hallucination rate estimator on common natural language in-context learning tasks using the Llama-2 family of LLMs [42]. We also provide results for Gemma-2 9B in Appendix G.2.1. As we no longer have access to the true f^* in this setting and can’t calculate the reference THR, we propose the Model Hallucination Rate (MHR) below as an analogous metric



(a) Model Hallucination Rate (MHR) and Posterior Hallucination Rate (PHR) with $\epsilon = 0.05$ as a function of the number of in-context examples. PHR closely follows MHR for all tasks.



(b) Error Rate and PHR with $\epsilon = 0.75$. PHR matches the error rate for SST2, Subjectivity, and AG News. However, for more difficult tasks like Medical QP and entailment tasks (RTE and WNLI), PHR is less accurate, highlighting the limitations of Llama-2-7b.

Figure 4: Performance Metrics for Llama-2-7b Across Tasks.

to evaluate the PHR against. We also evaluate against the empirical error rate given ground truth responses.

Setup. We consider tasks defined by six datasets: *Stanford Sentiment Treebank (SST2)* [49], *Subjectivity* [50], *AG News* [6], *Medical QP* [51], *RTE* [52], and *WNLI* [53]. We filter out any queries of length longer than 116 tokens. Descriptions of all data sets and pre-processing are given in Appendix F.2.

To implement ICL for a given dataset, we sample a response balanced training set of query/response pairs $\mathcal{D}_n = (x_i, y_i)_1^n$. We generate a response y from the predictive distribution given by a LLM $p_\theta(y | \mathcal{D}_n, x)$. We structure the prompt by adding strings to distinguish between inputs and labels. An example prompt from the Subjectivity dataset is shown in Appendix E.2.

Evaluation metrics. It is a challenge to assess the accuracy of the the posterior hallucination rate on LLM tasks as we only have a single ground truth labeled response for each query x instead of the ground truth f^* .

One idea is to use the empirical error rate to evaluate the model,

$$\hat{E}(x, y; p_\theta, \mathcal{D}_n) := \frac{1}{K} \sum_{i=1}^K \mathbb{1}\{y_i \neq y\}, \quad y_i \sim p_\theta(\cdot | x, \mathcal{D}_n). \quad (9)$$

However, this metric only provides a partial picture as it does not account for the inherent variety over responses given a mechanism, which would not constitute a hallucinations.

To get a more complete picture, we invoke Doob’s theorem and note that, when $(x_i, y_i) \sim p(x, y | f^*)$ and for sufficiently large N , we have

$$p(y | x, f^*) = p(y | x, (x_i, y_i)_1^\infty) \approx p(y | x, (x_i, y_i)_1^N) \approx p_\theta(y | x, (x_i, y_i)_1^N). \quad (10)$$

This motivates us to estimate the reference THR by approximating $p(y | x, f^*)$ with $p_\theta(y | x, \mathcal{D}_n \cup \mathcal{D}_{\text{eval}})$, where $\mathcal{D}_{\text{eval}}$ is a set of additional (x_i, y_i) examples from the task that are not in \mathcal{D}_n . We call this estimate the *model hallucination rate* (MHR) as it is derived under the model p_θ . Formally,

$$\text{MHR}(x; p_\theta, \mathcal{D}_n, \mathcal{D}_{\text{eval}}) := \frac{1}{K} \sum_{i=1}^K \mathbb{1}\left\{ \log p_\theta(y_i | x, \mathcal{D}_n \cup \mathcal{D}_{\text{eval}}) < \hat{Q}_\epsilon^{\text{eval}} \right\},$$

where $y_i \sim p_\theta(y | x, \mathcal{D}_n)$, K is the number of response samples, and $\hat{Q}_\epsilon^{\text{eval}}$ is the ϵ quantile of the samples $\{\log p_\theta(y_j | x, \mathcal{D}_n \cup \mathcal{D}_{\text{eval}})\}$ with $y_j \sim p_\theta(y | x, \mathcal{D}_n \cup \mathcal{D}_{\text{eval}})$. This value is only proposed

for model evaluating the model. It cannot be used to replace the PHR, as it depends on $\mathcal{D}_{\text{eval}}$, which is not available at test time. Intuitively the MHR computes the probability that an answer y given by a model that knows \mathcal{D}_n is considered a hallucination by a model that knows \mathcal{D}_n and $\mathcal{D}_{\text{eval}}$. As the model hallucination rate is an estimate of the true hallucination rate, we would like the posterior hallucination rate to be close to it.

For each task and context length $n \in [2, 4, 8, 16, 32]$ we sample 50 random training datasets \mathcal{D}_n , 50 random evaluation datasets $\mathcal{D}_{\text{eval}}$, and 10 random test samples. We report the mean squared error (MSE), regression coefficient β , p -value, and coefficient of determination (R^2) of the posterior hallucination rate as a linear predictor against both the error rate and MHR over all 50×10 test samples at each context length.

Results. We report results for Llama-2-7b. We set $N - n = 5$, $M = 10$, and $K = 50$. The top plots in Figure 4 show the MHR and estimated posterior hallucination rate against the number of in-context examples with $\epsilon = 0.05$. It shows that the posterior hallucination rate is a good estimator of the MHR. We show that this trend holds for alternative settings of ϵ in Figure 18 of Appendix G.2.2.

The bottom plots in Figure 4 show the empirical error rate and estimated posterior hallucination rate against the number of in-context examples with $\epsilon = 0.75$. The plots show that for SST, Subjective and AG News the PHR follows the error rate closely but disagrees with Medical QP, RTE and WNLI. We use a high value of epsilon so that only responses with very high probability are not taken to be hallucinations. This makes sense for the error rate as we care strictly about correctness rather than modeling the distribution. We ablate the ϵ parameter and report results in Figure 19 of Appendix G.

Discussion. The results highlight the usefulness of the PHR by demonstrating its ability to assess the model’s uncertainty in language tasks and predict its error rate without requiring an evaluation dataset. Additionally, the discrepancy between the PHR and error rate in Medical QP, RTE, and WNLI can be attributed to the model’s limited generalization in these tasks. This leads to an inadequate approximation of the posterior predictive: $p_\theta(y \mid x, \mathcal{D}_n) \not\approx p(y \mid x, \mathcal{D}_n)$. This inadequacy is supported by Figure 4, which shows that in tasks where the PHR does not align with the error rate (green line), the model’s performance is close to random guessing (dashed gray line). Hence the poor performance of the PHR in this scenarios is expected because our method relies on accurately approximating the posterior predictive and only accounts for hallucinations when the data distribution is properly modeled.

4 Conclusion

In this work, we have presented a new method for predicting the hallucination rate of in-context learning with conditional generative models. We provide a theoretical justification for our method. In synthetic experiments, we demonstrate that the PHR estimator yields accurate estimates of the true probability of hallucination. With pre-trained LLMs, we demonstrate that it is valuable for predicting the error rate of “in-capability” natural language ICL tasks.

High-fidelity estimation of the PHR relies on two strong assumptions. The first is that the in-context learning problem data admits a de Finetti representation; the second is that the CGM p_θ is a faithful estimate of the true distribution p_{ICL} . While our results offer support for the adoption of these assumptions, we also demonstrate that even minor divergences between p_θ and p_{ICL} can result in underestimation. Falck et al. [41] also report instances where properties of the predictive distribution of a pre-trained LLM significantly diverge from those of the true Bayesian posterior predictive distribution for synthetic ICL tasks. These findings highlight a challenge in using PHR as a decision support tool and point to future work on improving the robustness of the PHR estimator or the optimization of conditional generative models for in-context learning.

5 Acknowledgements

The authors would like to thank Amir Feder, Alessandro Grande, Achille Nazaret, Yookoon Park, Kathy Perez, Sebastian Salazar, Claudia Shi, Brian Trippe, Al Tucker, and Luhuan Wu for their reviews, feedback, and support.

References

- [1] Tom Brown, Benjamin Mann, Nick Ryder, Melanie Subbiah, Jared D Kaplan, Prafulla Dhariwal, Arvind Neelakantan, Pranav Shyam, Girish Sastry, Amanda Askell, et al. Language models are few-shot learners. *NeurIPS*, 33:1877–1901, 2020.
- [2] Qingxiu Dong, Lei Li, Damai Dai, Ce Zheng, Zhiyong Wu, Baobao Chang, Xu Sun, Jingjing Xu, and Zhifang Sui. A survey on in-context learning. *arXiv:2301.00234*, 2022.
- [3] Machel Reid, Nikolay Savinov, Denis Teplyashin, Dmitry Lepikhin, Timothy Lillicrap, Jean-baptiste Alayrac, Radu Soricut, Angeliki Lazaridou, Orhan Firat, Julian Schrittwieser, et al. Gemini 1.5: Unlocking multimodal understanding across millions of tokens of context. *arXiv:2403.05530*, 2024.
- [4] Abdul Fatir Ansari, Lorenzo Stella, Caner Turkmen, Xiyuan Zhang, Pedro Mercado, Huibin Shen, Oleksandr Shchur, Syama Sundar Rangapuram, Sebastian Pineda Arango, Shubham Kapoor, et al. Chronos: Learning the language of time series. *arXiv:2403.07815*, 2024.
- [5] Joshua Maynez, Shashi Narayan, Bernd Bohnet, and Ryan McDonald. On faithfulness and factuality in abstractive summarization. In *ACL*, pages 1906–1919, Online, July 2020.
- [6] Xiang Zhang, Junbo Zhao, and Yann LeCun. Character-level convolutional networks for text classification. *NeurIPS*, 2015.
- [7] Samuel Müller, Noah Hollmann, Sebastian Pineda Arango, Josif Grabocka, and Frank Hutter. Transformers can do Bayesian inference. In *ICLR*, 2021.
- [8] Sang Michael Xie, Aditi Raghunathan, Percy Liang, and Tengyu Ma. An explanation of in-context learning as implicit Bayesian inference. In *ICLR*, 2021.
- [9] Philip Feldman, James R Foulds, and Shimei Pan. Trapping LLM hallucinations using tagged context prompts. *arXiv:2306.06085*, 2023.
- [10] Shuo Zhang, Liangming Pan, Junzhou Zhao, and William Yang Wang. Mitigating language model hallucination with interactive question-knowledge alignment. *arXiv:2305.13669*, 2023.
- [11] Baolin Peng, Michel Galley, Pengcheng He, Hao Cheng, Yujia Xie, Yu Hu, Qiuyuan Huang, Lars Liden, Zhou Yu, Weizhu Chen, et al. Check your facts and try again: Improving large language models with external knowledge and automated feedback. *arXiv:2302.12813*, 2023.
- [12] Nouha Dziri, Andrea Madotto, Osmar R Zaiane, and Avishek Joey Bose. Neural path hunter: Reducing hallucination in dialogue systems via path grounding. In *EMNLP*, pages 2197–2214, 2021.
- [13] Luyu Gao, Zhuyun Dai, Panupong Pasupat, Anthony Chen, Arun Tejasvi Chaganty, Yicheng Fan, Vincent Zhao, Ni Lao, Hongrae Lee, Da-Cheng Juan, et al. RARR: Researching and revising what language models say, using language models. In *ACL*, pages 16477–16508, 2023.
- [14] Xingxuan Li, Ruochen Zhao, Yew Ken Chia, Bosheng Ding, Shafiq Joty, Soujanya Poria, and Lidong Bing. Chain-of-knowledge: Grounding large language models via dynamic knowledge adapting over heterogeneous sources. In *ICLR*, 2023.
- [15] Neeraj Varshney, Wenlin Yao, Hongming Zhang, Jianshu Chen, and Dong Yu. A stitch in time saves nine: Detecting and mitigating hallucinations of LLMs by validating low-confidence generation. *arXiv:2307.03987*, 2023.
- [16] Dan Su, Xiaoguang Li, Jindi Zhang, Lifeng Shang, Xin Jiang, Qun Liu, and Pascale Fung. Read before generate! Faithful long form question answering with machine reading. In *ACL*, pages 744–756, 2022.
- [17] Yung-Sung Chuang, Yujia Xie, Hongyin Luo, Yoon Kim, James R Glass, and Pengcheng He. Dola: Decoding by contrasting layers improves factuality in large language models. In *ICLR*, 2024.

- [18] Nayeon Lee, Wei Ping, Peng Xu, Mostofa Patwary, Pascale N Fung, Mohammad Shoeybi, and Bryan Catanzaro. Factuality enhanced language models for open-ended text generation. *NeurIPS*, 35:34586–34599, 2022.
- [19] Weijia Shi, Xiaochuang Han, Mike Lewis, Yulia Tsvetkov, Luke Zettlemoyer, and Wen-tau Yih. Trusting your evidence: Hallucinate less with context-aware decoding. In *Proceedings of the 2024 Conference of the North American Chapter of the Association for Computational Linguistics: Human Language Technologies (Volume 2: Short Papers)*, pages 783–791, 2024.
- [20] Sabrina J Mielke, Arthur Szlam, Emily Dinan, and Y-Lan Boureau. Reducing conversational agents’ overconfidence through linguistic calibration. *TACL*, 10:857–872, 2022.
- [21] Stephanie Lin, Jacob Hilton, and Owain Evans. Teaching models to express their uncertainty in words. *TMLR*, 2023.
- [22] Neil Band, Xuechen Li, Tengyu Ma, and Tatsunori Hashimoto. Linguistic calibration of language models. *arXiv:2404.00474*, 2024.
- [23] Samuel Marks and Max Tegmark. The geometry of truth: Emergent linear structure in large language model representations of true/false datasets, 2023.
- [24] Amos Azaria and Tom Mitchell. The internal state of an LLM knows when it’s lying. In *EMNLP*, pages 967–976, 2023.
- [25] Collin Burns, Haotian Ye, Dan Klein, and Jacob Steinhardt. Discovering latent knowledge in language models without supervision. In *ICLR*, 2022.
- [26] Kenneth Li, Oam Patel, Fernanda Viégas, Hanspeter Pfister, and Martin Wattenberg. Inference-time intervention: Eliciting truthful answers from a language model. *NeurIPS*, 36, 2024.
- [27] Nina Rimskey, Nick Gabrieli, Julian Schulz, Meg Tong, Evan Hubinger, and Alexander Matt Turner. Steering Llama 2 via contrastive activation addition. *arXiv:2312.06681*, 2023.
- [28] Junyu Luo, Cao Xiao, and Fenglong Ma. Zero-resource hallucination prevention for large language models. *CoRR*, 2023.
- [29] Niels Mündler, Jingxuan He, Slobodan Jenko, and Martin Vechev. Self-contradictory hallucinations of large language models: Evaluation, detection and mitigation. In *ICLR*, 2024.
- [30] Shehzaad Dhuliawala, Mojtaba Komeili, Jing Xu, Roberta Raileanu, Xian Li, Asli Celikyilmaz, and Jason E Weston. Chain-of-verification reduces hallucination in large language models. In *ICLR 2024 Workshop on Reliable and Responsible Foundation Models*, 2024.
- [31] Tianyi Zhang, Varsha Kishore, Felix Wu, Kilian Q Weinberger, and Yoav Artzi. BERTScore: Evaluating text generation with BERT. In *ICLR*, 2019.
- [32] Saurav Kadavath, Tom Conerly, Amanda Askell, Tom Henighan, Dawn Drain, Ethan Perez, Nicholas Schiefer, Zac Hatfield Dodds, Nova DasSarma, Eli Tran-Johnson, et al. Language models (mostly) know what they know. *arXiv:2207.05221*, 2022.
- [33] Lorenz Kuhn, Yarin Gal, and Sebastian Farquhar. Semantic uncertainty: Linguistic invariances for uncertainty estimation in natural language generation. In *ICLR*, 2023.
- [34] Zhen Lin, Shubhendu Trivedi, and Jimeng Sun. Generating with confidence: Uncertainty quantification for black-box large language models. *TMLR*, 2024.
- [35] Jiuhai Chen and Jonas Mueller. Quantifying uncertainty in answers from any language model and enhancing their trustworthiness. In *ACL*, pages 5186–5200, 2024.
- [36] Mohamed Elaraby, Mengyin Lu, Jacob Dunn, Xueying Zhang, Yu Wang, and Shizhu Liu. Halo: Estimation and reduction of hallucinations in open-source weak large language models. *arXiv:2308.11764*, 2023.
- [37] Potsawee Manakul, Adian Liusie, and Mark JF Gales. SelfCheckGPT: Zero-resource black-box hallucination detection for generative large language models. In *EMNLP*, 2023.

- [38] Jeremy R Cole, Michael JQ Zhang, Daniel Gillick, Julian Martin Eisenschlos, Bhuwan Dhingra, and Jacob Eisenstein. Selectively answering ambiguous questions. *EMNLP*, 2023.
- [39] Edwin Fong, Chris Holmes, and Stephen G Walker. Martingale posterior distributions. *Journal of the Royal Statistical Society Series B: Statistical Methodology*, 85(5):1357–1391, 2023.
- [40] Hyungi Lee, Eunggu Yun, Giung Nam, E Fong, and Juho Lee. Martingale posterior neural processes. In *ICLR*. ICLR, 2023.
- [41] Fabian Falck, Ziyu Wang, and Christopher C Holmes. Is in-context learning in large language models Bayesian? A martingale perspective. In *ICML*, 2024.
- [42] Hugo Touvron, Louis Martin, Kevin Stone, Peter Albert, Amjad Almahairi, Yasmine Babaei, Nikolay Bashlykov, Soumya Batra, Prajjwal Bhargava, Shruti Bhosale, et al. Llama 2: Open foundation and fine-tuned chat models. *arXiv:2307.09288*, 2023.
- [43] Gemma Team. Gemma, 2024.
- [44] Ashish Vaswani, Noam Shazeer, Niki Parmar, Jakob Uszkoreit, Llion Jones, Aidan N Gomez, Łukasz Kaiser, and Illia Polosukhin. Attention is all you need. *NeurIPS*, 2017.
- [45] Naimeng Ye, Hanming Yang, Andrew Siah, and Hongseok Namkoong. Pre-training and in-context learning is Bayesian inference a la de Finetti. *arXiv:2408.03307*, 2024.
- [46] Edwin Shields Hewitt and Leonard J. Savage. Symmetric measures on cartesian products. *Transactions of the American Mathematical Society*, 80:470–501, 1955.
- [47] Joseph L Doob. Application of the theory of martingales. *Le calcul des probabilités et ses applications*, pages 23–27, 1949.
- [48] Marta Garnelo, Dan Rosenbaum, Christopher Maddison, Tiago Ramalho, David Saxton, Murray Shanahan, Yee Whye Teh, Danilo Rezende, and SM Ali Eslami. Conditional neural processes. In *ICML*, pages 1704–1713, 2018.
- [49] Richard Socher, Alex Perelygin, Jean Wu, Jason Chuang, Christopher D. Manning, Andrew Ng, and Christopher Potts. Recursive deep models for semantic compositionality over a sentiment treebank. In *EMNLP*, pages 1631–1642, 2013.
- [50] Sida Wang and Christopher D. Manning. Baselines and bigrams: simple, good sentiment and topic classification. In *ACL*, page 90–94, 2012.
- [51] Clara H McCreery, Namit Katariya, Anitha Kannan, Manish Chablani, and Xavier Amatriain. Effective transfer learning for identifying similar questions: Matching user questions to covid-19 faqs. In *Proceedings of the 26th ACM SIGKDD international conference on knowledge discovery & data mining*, pages 3458–3465, 2020.
- [52] Ido Dagan, Oren Glickman, and Bernardo Magnini. The pascal recognising textual entailment challenge. In Joaquin Quiñero-Candela, Ido Dagan, Bernardo Magnini, and Florence d’Alché Buc, editors, *Machine Learning Challenges. Evaluating Predictive Uncertainty, Visual Object Classification, and Recognising Tectual Entailment*, pages 177–190, Berlin, Heidelberg, 2006. Springer Berlin Heidelberg. ISBN 978-3-540-33428-6.
- [53] Hector J. Levesque, Ernest Davis, and Leora Morgenstern. The winograd schema challenge. In Gerhard Brewka, Thomas Eiter, and Sheila A. McIlraith, editors, *KR*. AAAI Press, 2012. ISBN 978-1-57735-560-1.
- [54] Ferenc Huszár. Implicit Bayesian inference in large language models, 2023. Online; accessed 10-July-2023.
- [55] Michael Hahn and Navin Goyal. A theory of emergent in-context learning as implicit structure induction. *arXiv:2303.07971*, 2023.
- [56] Hui Jiang. A latent space theory for emergent abilities in large language models. *arXiv:2304.09960*, 2023.

- [57] Yufeng Zhang, Fengzhuo Zhang, Zhuoran Yang, and Zhaoran Wang. What and how does in-context learning learn? Bayesian model averaging, parameterization, and generalization. *arXiv:2305.19420*, 2023.
- [58] Johannes Von Oswald, Eyvind Niklasson, Ettore Randazzo, João Sacramento, Alexander Mordvintsev, Andrey Zhmoginov, and Max Vladymyrov. Transformers learn in-context by gradient descent. In *ICML*, 2023.
- [59] Ekin Akyürek, Dale Schuurmans, Jacob Andreas, Tengyu Ma, and Denny Zhou. What learning algorithm is in-context learning? Investigations with linear models. In *ICLR*, 2023.
- [60] Chi Han, Ziqi Wang, Han Zhao, and Heng Ji. In-context learning of large language models explained as kernel regression. *arXiv:2305.12766*, 2023.
- [61] Roei Hendel, Mor Geva, and Amir Globerson. In-context learning creates task vectors. In *EMNLP*, 2023.
- [62] Eric Todd, Millicent L Li, Arnab Sen Sharma, Aaron Mueller, Byron C Wallace, and David Bau. Function vectors in large language models. In *ICLR*, 2024.
- [63] Jiachang Liu, Dinghan Shen, Yizhe Zhang, Bill Dolan, Lawrence Carin, and Weizhu Chen. What makes good in-context examples for GPT-3? In *Proceedings of Deep Learning Inside Out (DeeLIO 2022): The 3rd Workshop on Knowledge Extraction and Integration for Deep Learning Architectures*, 2022.
- [64] Yao Lu, Max Bartolo, Alastair Moore, Sebastian Riedel, and Pontus Stenetorp. Fantastically ordered prompts and where to find them: Overcoming few-shot prompt order sensitivity. In *ACL*, 2022.
- [65] Zihao Zhao, Eric Wallace, Shi Feng, Dan Klein, and Sameer Singh. Calibrate before use: Improving few-shot performance of language models. In *ICML*, 2021.
- [66] Jannik Kossen, Yarin Gal, and Tom Rainforth. In-context learning learns label relationships but is not conventional learning. In *ICLR*, 2024.
- [67] Jerry Wei, Jason Wei, Yi Tay, Dustin Tran, Albert Webson, Yifeng Lu, Xinyun Chen, Hanxiao Liu, Da Huang, Denny Zhou, et al. Larger language models do in-context learning differently. *arXiv:2303.03846*, 2023.
- [68] Yasaman Razeghi, Robert L Logan IV, Matt Gardner, and Sameer Singh. Impact of pretraining term frequencies on few-shot reasoning. In *EMNLP*, 2022.
- [69] Jane Pan, Tianyu Gao, Howard Chen, and Danqi Chen. What in-context learning "learns" in-context: Disentangling task recognition and task learning. In *ACL*, 2023.
- [70] Rishabh Agarwal, Avi Singh, Lei M Zhang, Bernd Bohnet, Luis Rosias, Stephanie CY Chan, Biao Zhang, Aleksandra Faust, and Hugo Larochelle. Many-shot in-context learning. In *ICML 2024 Workshop on In-Context Learning*, 2024.
- [71] Josh Achiam, Steven Adler, Sandhini Agarwal, Lama Ahmad, Ilge Akkaya, Florencia Leoni Aleman, Diogo Almeida, Janko Altschmidt, Sam Altman, Shyamal Anadkat, et al. GPT-4 technical report. *arXiv:2303.08774*, 2023.
- [72] Jinhao Duan, Hao Cheng, Shiqi Wang, Chenan Wang, Alex Zavalny, Renjing Xu, Bhavya Kailkhura, and Kaidi Xu. Shifting attention to relevance: Towards the uncertainty estimation of large language models. *arXiv:2307.01379*, 2023.
- [73] Gustaf Ahlritz, Tian Qin, Nikhil Vyas, Boaz Barak, and Benjamin L Edelman. Distinguishing the knowable from the unknowable with language models. In *ICML*, 2024.
- [74] Daniel D Johnson, Daniel Tarlow, David Duvenaud, and Chris J Maddison. Experts don't cheat: Learning what you don't know by predicting pairs. *arXiv:2402.08733*, 2024.

- [75] Zhiyuan Hu, Chumin Liu, Xidong Feng, Yilun Zhao, See-Kiong Ng, Anh Tuan Luu, Junxian He, Pang Wei Koh, and Bryan Hooi. Uncertainty of thoughts: Uncertainty-aware planning enhances information seeking in large language models. In *ICLR 2024 Workshop on Large Language Model (LLM) Agents*, 2024.
- [76] Hong Jun Jeon, Jason D Lee, Qi Lei, and Benjamin Van Roy. An information-theoretic analysis of in-context learning. In *ICML*, 2024.
- [77] Katherine Tian, Eric Mitchell, Huaxiu Yao, Christopher D Manning, and Chelsea Finn. Fine-tuning language models for factuality. In *ICLR*, 2024.
- [78] Marta Garnelo, Jonathan Schwarz, Dan Rosenbaum, Fabio Viola, Danilo J Rezende, SM Eslami, and Yee Whye Teh. Neural processes. *ICML 2018 workshop on Theoretical Foundations and Applications of Deep Generative Models*, 2018.
- [79] Hyunjik Kim, Andriy Mnih, Jonathan Schwarz, Marta Garnelo, Ali Eslami, Dan Rosenbaum, Oriol Vinyals, and Yee Whye Teh. Attentive neural processes. In *ICLR*, 2019.
- [80] Tung Nguyen and Aditya Grover. Transformer neural processes: Uncertainty-aware meta learning via sequence modeling. In *ICML*, 2022.
- [81] Jason Wei, Xuezhi Wang, Dale Schuurmans, Maarten Bosma, Fei Xia, Ed Chi, Quoc V Le, Denny Zhou, et al. Chain-of-thought prompting elicits reasoning in large language models. *NeurIPS*, pages 24824–24837, 2022.
- [82] Ilya Loshchilov and Frank Hutter. Decoupled weight decay regularization, 2019.

A Related Works

Mechanisms and Capabilities of ICL. Several papers argue that ICL can theoretically and in synthetic scenarios implement learning principles like Bayesian inference or gradient descent [8, 54–59]. Evidence in actual pre-trained LLMs shows that ICL can be approximated as a kernel regression [60], and parametric approximations to ICL can be derived from the hidden state of the last input demonstration [61, 62]. Practical shortcomings of ICL include dependence on example order [63–66] and the impact of prediction preferences acquired during pre-training [65–69]. While future models might improve ICL performance [70], current limitations are clear and are thoroughly investigated in recent work by Falck et al. [41]. These results imply that ICL in real LLMs does not implement perfect Bayesian inference but suggest that LLM predictive uncertainty includes both epistemic and aleatoric components, and LLMs can update uncertainties with new observations.

Uncertainties in LLMs. Our results are supported by evidence that predictive uncertainties of large language models are well-calibrated, even in scenarios requiring epistemic uncertainty [32, 71]. Relatedly, LLM uncertainties have been used to detect hallucinations in free-form generation settings such as question-answering [28–30, 32–38, 72]. Although not all these papers explicitly focus on LLM uncertainties, they rely on it implicitly by sampling multiple model completions for a query and quantifying the differences in meaning. Specifically, Kuhn et al. [33] highlight the challenge of isolating uncertainty over semantic meaning from uncertainty over syntax or lexis in free-form generation tasks. While these approaches do not disambiguate aleatoric and epistemic uncertainty, Ahdriz et al. [73], Johnson et al. [74] recently proposed methods to do so in CGMs. However, Ahdriz et al. [73] require access to two LLMs of different parameter counts, and Johnson et al. [74] do not apply their method to LLMs. Additionally, Hu et al. [75] show that Bayesian experimental design can turn LLMs into strategic question askers, and Jeon et al. [76] present a theoretic study on sources of errors in ICL.

Hallucinations in LLMs. In addition to approaches based on uncertainty, a variety of other strategies have been explored to detect or mitigate hallucinations in LLMs: retrieval-augmented generation [9–16], custom token sampling procedures [17–19], model fine-tuning to improve uncertainties [20–22] or reduce hallucinations outright [77], as well as learning to extract or steer truthfulness from hidden states [23–27].

Neural processes. Neural processes (NPs) [48, 78–80] are neural network-based non-parametric models trained over a collection of datasets. Similar to ICL, NPs take a collection of datapoints as input and amortize task learning in a single forward pass through the model. For instance, when datasets are drawn from a Gaussian process prior, NPs’ predictive distributions closely approximate the true Bayesian posterior predictive for a given input dataset [7]. NPs have been used successfully for tasks requiring reliable uncertainty estimation, such as Bayesian optimization [40, 78, 80] or active feature acquisition [48]. Recently, Lee et al. [40] applied Doob’s theorem to quantify uncertainties in neural processes.

Martingale Posterior The work closest in spirit to ours is [39] which proposes Martingale Posterior distributions. The idea of that paper is to use the posterior predictive, and not the posterior as the main object for expressing uncertainty. As in this paper, samples from the posterior predictive are used to estimate quantities of interest. Then, by repeated resampling and estimation of the predictive, one obtains a “posterior” over the estimate. Falck et al. [41] work to formalize this methodology for LLMs. They propose a set of statistical tests to estimate whether an LLM satisfies the “Martingale property.” These tests depend on being able to sample from the true Bayesian model that defines the posterior predictive distribution estimated by the LLM predictive distribution. In their evaluations using synthetic data and pre-trained LLMs, they find that violations of the Martingale property can occur. Moreover, they find that the fidelity of the LLM predictive distribution to the true Bayesian posterior predictive decreases as the length of dataset completions ($N - n$) increases. They also derive an epistemic uncertainty estimator based on the posterior covariance over mechanisms, which has connections to the posterior hallucination rate and the mutual information estimand we propose in Appendix D.

B Further Discussion

B.1 Broader Social Impact

Positive social impact. Our work allows for greater interpretability into the responses produced by LLMs and hallucination rate prediction. Being able to discern when a Large Language Model (LLM) is likely to hallucinate is crucial for several reasons, particularly concerning its social impact. In terms of misinformation, if users cannot distinguish between accurate information and hallucinations, they may spread misinformation unknowingly. This can damage the credibility of the platforms using LLMs and the trust users place in AI systems. Further, as LLMs become more commonplace in high-risk sectors like medicine or finance, hallucinated medical advice can be dangerous, leading to harmful health practices or delayed treatment, while erroneous financial information can lead to poor investments or financial loss. Ethically, hallucinations can reinforce or propagate biases and stereotypes if the generated content reflects societal prejudices. This can perpetuate discrimination and inequality. Understanding when hallucinations are likely to occur is vital for holding developers and companies accountable for the content their models produce. Finally, many researchers use LLMs and other CGMs to generate or label data. Hallucinations in this setting can lead to false discoveries and wasted resources.

Being able to accurately predict hallucination rates for given tasks is essential for ensuring that AI systems contribute positively to society. It allows for maintaining trust, safety, ethical standards, and the overall integrity of information dissemination.

Negative social impact. When our model is being used as intended but gives incorrect results (i.e. produces a low estimate of probability of hallucination when the true probability is high), it could inadvertently be reinforcing biases present in hallucinations while increasing user trust in the outputs.

B.2 What kind of uncertainty does the posterior hallucination rate quantify?

Building trustworthy and effective ICL solutions requires understanding why and when incorrect or unexpected responses are generated by a CGM. The ICL literature provides two findings that suggest distinct sources of hallucination.

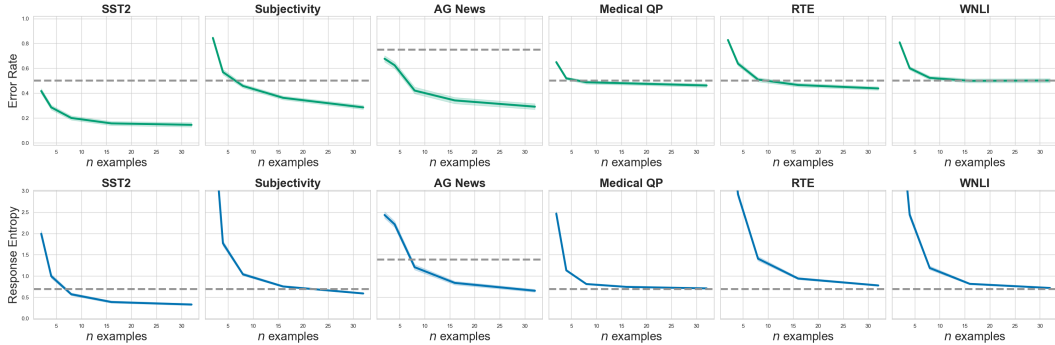


Figure 5: **Llama-2-7b**: Error Rate (Top green curves) and Response Entropy (Bottom blue curves) on LLM in-context learning tasks. Grey dashed lines represent the error rate and entropy of a random classifier over the set of valid responses.

The first finding is that error rate and prediction entropy decreases and saturates with an increasing number of examples [66]. This trend is illustrated in Figure 5 using the Llama-2-7b model [42] on a set of natural language ICL tasks. This finding indicates that one source of hallucination is an insufficient number of relevant in-context examples.

The second finding from the literature is that there are still many tasks for which ICL performs poorly. For example, the response accuracy of Gemini Pro 1.5 given several in-context examples from the American Mathematics Competition is only 37.2%, implying that the model would hallucinate an incorrect response at a rate of 62.8% [3]. We hypothesize that regardless of the number of relevant in-context examples, the model may lack the capacity to answer a specific user query from a complex or new domain accurately. This hypothesis is illustrated using Llama-2-7B by comparing the graphs

of the first three tasks (SST2 [49], Subjective [50], and AG News [6]) to the graph of the WNLI task [53]) in Figure 5. While the error rate and response entropy for each of the first three tasks improves significantly over random guessing with more examples, both measures appear to saturate near the random baseline for the WNLI task. The second source of hallucinations is then associated with whether a model has the capacity to factually answer queries for an ICL task.

This work focuses on the first source of hallucinations. That is, the *posterior hallucination rate* is concerned with estimating the rate of hallucinations that stem from a lack of relevant context, and not those that stem from a lack of model capacity. The predictive distribution encodes response variety coming from several sources, and this variety is closely tied to the ways in which a model can generate a hallucination. We discuss these sources of response variety—or uncertainty—below and their relation to hallucinations and the posterior hallucination rate.

Aleatoric Uncertainty. The $(1 - \epsilon)$ -likely set defined by a given mechanism f^* reflects an irreducible component of response uncertainty. To illustrate the concept of irreducible (sometimes called “aleatoric”) response uncertainty, imagine an LLM fit to vast corpora containing many calculus examples such that it has the capacity for integration. Consider,

Prompt 1:

fill in the blanks: the integral of x^2 with respect to x on the interval $[-3, 3]$ is \square .

If an LLM effectively models the mechanism associated with integration datasets, then response variety will be determined by all the different ways the model can generate the correct response: e.g., 18, eighteen, $\frac{3^3}{3} - \frac{-3^3}{3}$, $9 + 9$, $2 * 9$, XVIII, etc. Uncertainty reflecting the plurality of ways to communicate the same meaning is commonly referred to as *syntactic uncertainty* [33], which is considered irreducible in this particular example. However, in language tasks, irreducible uncertainty need not be syntactic by necessity.

To enrich this concept, consider the same LLM and

Prompt 2:

fill in the blanks: the integral of \square , with respect to x on the interval $[-3, 3]$ is \square .

In addition to the syntactically different ways to specify a particular function (x^2 , x squared, xx , ...) and the corresponding result (18, eighteen, XVIII, ...), response variety also depends on the semantically different integrands that could fill the first blank (x^3 , $\cos(x)$, $\exp(x)$, $2xy$, ...) and the semantically different possible results. This additional variety is emblematic of *semantic uncertainty* [33]. However, while high semantic uncertainty can be indicative of hallucinations, it is not a problem in this example because the imputation of any sensible function and answer could still be valid under the mechanism associated with integration datasets. That is, given *Prompt 2*, uncertainty over semantically different functions is expected and even desirable.

This pair of examples illustrate an important insight; *irreducible uncertainty is mechanism relative*. If, for example, we are in a simple question answering setting and the mechanism defines a $(1 - \epsilon)$ -likely set over correct responses, then, equivocating irreducible and syntactic uncertainty may be appropriate. However, in the second example we show that this decomposition is not necessarily appropriate.

Type I epistemic uncertainty. We return to *Prompt 1* and give two examples that illustrate an uncertainty about mechanisms f that is reducible. First, consider a setting where the user desires the response in terms of a reduced fraction. There are two obvious ways that the user could augment *Prompt 1* to reduce the uncertainty over mechanisms yielding integer, word, fraction, etc. responses. (1) the user could simply replace “fill in the blanks” with “fill in the blank with a reduced fraction.” (2) the user could take an ICL approach and augment the prompt with a number of examples:

Prompt 3:

Input: the integral of x^3 with respect to x on the interval $[-1, 6]$

Label: $\frac{1295}{4}$

Input: the integral of x^6 with respect to x on the interval $[-2, 2]$

Label: $0 / 7$.

Input: the integral of x^2 with respect to x on the interval $[-3, 3]$

Label:

The first choice may result in reducing all uncertainty about which mechanism to sample responses from. For the second choice, we can imagine a progressive reduction in uncertainty about the appropriate mechanism as more examples are added in-context. For example, if we were to see the two provided examples, we may still be uncertain about whether to respond with a number or a fraction, or whether to respond with any correct fraction or the reduced fraction. For example, given the context, a response of $\frac{54}{3}$ would be as plausible as the desired $\frac{18}{1}$. It may not be until the prompt included an example like, “the integral of x^3 with respect to x on the interval $[2, 4]$ is $60/1$,” until all uncertainty about the mechanism is resolved. We propose that this explains why we see a reduction in the error rate and response entropy in a task like WNLI that is “out-of-capacity” for Llama-2-7B. That is, as we provide more in-context examples, the predictive distribution can be more aligned with the set of acceptable responses, even though those responses may still be incorrect.

The preceding example illustrated a hallucination as a misaligned response, now let’s turn to an example of a non-factual response. Returning to *Prompt 1*, imagine now that the model generates the response 42. Why did it do this? A plausible answer could be that the model cannot do integration. We will touch on this possibility next, but first let’s consider an equally interesting case. We know from the few-shot and chain-of-thought prompting literature [14, 30, 81], that augmenting the context can have significant effects on ICL accuracy. For example, consider the hypothetical setting where the LLM has “grokked” algebra, but only has the superficial capacity to output a number when completing definite integrals. Or maybe the model has capacity to do integration, but the format of the examples and query is not common in the training corpora. The LLM then may actually have the capacity to answer the question given some clever prompting. For example,

Input: the integral of x^3 with respect to x on the interval $[-1, 6]$

Label: $6^4 / 4 - (-1)^4 / 4 = 1295 / 4$

Input: the integral of x^3 with respect to x on the interval $[2, 4]$

Label: $4^4 / 4 - 2^4 / 4 = 60 / 1$.

Prompt 4:

...

Input: the integral of x^6 with respect to x on the interval $[-2, 2]$

Label: $2^7 / 7 - (-2)^7 / 7 = 0 / 7$

Input: the integral of x^2 with respect to x on the interval $[-3, 3]$

Label:

Again, as the prompt contains more examples that translate the form of the query into a suitable format, we can expect that the uncertainty about the answer will reduce. For conditional models in general, we will call this *Type I epistemic uncertainty*, which could also be understood as in-context epistemic uncertainty. Both of these examples illustrate hallucinations that are due to insufficient context.

Type II epistemic uncertainty. Let’s return to *Prompt 1*, but this time imagine an LLM fit to a corpus *not* containing any examples from calculus or related mathematical fields. Or perhaps we could imagine an LLM with finite capacity that for whatever reason does not have the capacity to answer

integrals. What do we do when the model generates “Dua Lipa?” What do we do when the model outputs members of the set $\{17, 137, \text{Dua Lipa}, \text{Wednesday}, \dots\}$? We say that the response should have high *Type II epistemic uncertainty* because the LLM has not acquired the capacity to model the mechanism class, F , corresponding to integrals. This could also be understood as in-weights θ epistemic uncertainty. In the example of *Prompt 4*, imagine if there were no number of exemplars that could induce a correct response.

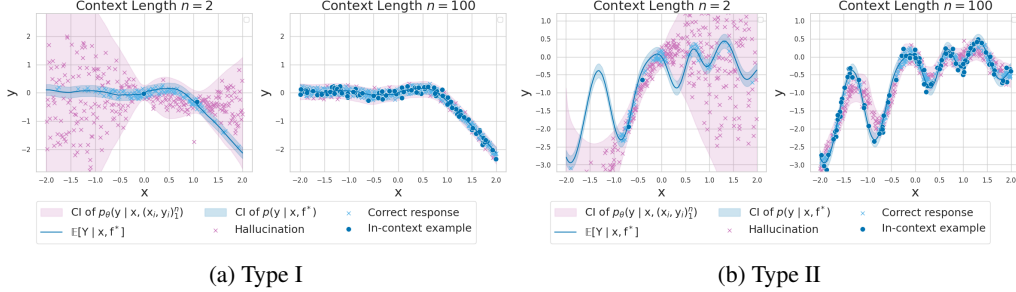


Figure 6: Comparing different sources of hallucination for regression models. Figure 6a illustrates hallucinations due to Type I epistemic uncertainty. As the context length increases, the predictive distribution concentrates around the true distribution and the model hallucinates less. Figure 6b illustrates hallucinations due to Type II epistemic uncertainty. Given data from an out-of-distribution function, the predictive distribution may not cover the true distribution. Moreover, the model still hallucinates significantly even when Type I epistemic uncertainty is minimized as the number of in-context examples is large.

When a condition generative model p_θ is a good estimator of the true distribution p , the posterior hallucination rate—and mutual information quantity we propose in Appendix D—are designed to estimate Type I epistemic uncertainty. We leave the important work of estimating the posterior hallucination rate when the CGM is not a good estimator (under Type II epistemic uncertainty) to future work.

C Proof of Theorems in Main Text

We begin by stating a lemma that will be useful throughout.

Lemma C.1. *Assume that the conditions of Theorem 1 hold for F and (X, Y) , then for a fixed dataset and query \mathcal{D}_n, x and under a probability model where $F \sim p(f \mid \mathcal{D}_n)$ and $(X_i, Y_i) \sim p(x, y \mid F)$, then*

$$\log p(Y \mid x, F) = \lim_{n \rightarrow \infty} \log p(Y \mid x, (X_i, Y_i)_1^n)$$

almost surely.

Proof. For a fixed y, x , let $g(f) = p(y \mid x, F)$ and then apply Doob’s theorem on the probability model. Then it is the case that

$$g(F) = \lim_{n \rightarrow \infty} \mathbb{E}_{F \sim p(f \mid \mathcal{D}_n)} [p(y \mid x, F) \mid (X_i, Y_i)_1^n] \quad (11)$$

$$= \lim_{n \rightarrow \infty} \int p(y \mid f, x) dP(f \mid (X_i, Y_i)_1^n) \quad (12)$$

$$= \lim_{n \rightarrow \infty} \int p(y \mid f, x) dP(f \mid (X_i, Y_i)_1^n, x) \quad (13)$$

$$= \lim_{n \rightarrow \infty} p(y \mid x, (X_i, Y_i)_1^n) \quad (14)$$

where Equation (13) holds because x is independent of F . Taking logs at both sides and using the continuity of the logarithm, we obtain

$$\log g(F) = \lim_{n \rightarrow \infty} \log p(y \mid x, (X_i, Y_i)_1^n)$$

and because this holds for all y , it must hold for the random variable Y . \square

Now we restate the main theorem with proof:

Theorem 3 (PHR via Posterior Predictive). *Assume that the conditions of Theorem 1 hold for F and X, Y , then,*

$$\begin{aligned} h_\epsilon(x) &= \iint \mathbb{1} \{ \log p(y | x, f) < Q_\epsilon(f, x) \} dP(y | \mathcal{D}_n, x) dP(f | \mathcal{D}_n) \\ &= \iint \mathbb{1} \left\{ \lim_{N \rightarrow \infty} \log p(y | (x_i, y_i)_1^N, x) < Q_\epsilon((x_i, y_i)_1^\infty, x) \right\} dP(y | \mathcal{D}_n, x) dP((x, y)_{n+1}^\infty | \mathcal{D}_n), \end{aligned}$$

where $Q_\epsilon((x_i, y_i)_1^\infty, x)$ is the ϵ -quantile of $\lim_{N \rightarrow \infty} \log p(Y | x, (x_i, y_i)_1^N)$ under the limiting distribution $\lim_{N \rightarrow \infty} p(Y | x, (x_i, y_i)_1^N)$.

Proof. Define an alternative probability model such that $F \sim p(f | \mathcal{D}_n)$ and $(X_i, Y_i) \sim p(x, y | F)$. Let $p_a, \mathbb{E}_a, Q_{a,\epsilon}$ and P_a denote the relevant quantities computed with respect to this alternative probability model.

First, note that by expanding the definition of $Q_{a,\epsilon}(f, x)$ under this new probability model

$$Q_{a,\epsilon}(F, x) = \inf \{ q \in \mathbb{R} : \epsilon \leq P_a(\log p_a(Y | x, F) \leq q | F, x) \} \quad (15)$$

$$Q_{a,\epsilon}(F, x) = \inf \{ q \in \mathbb{R} : \epsilon \leq P_a(\log p_a(Y | x, F) \leq q | F, x, (X, Y)_1^\infty) \} \quad (16)$$

$$= \inf \left\{ q \in \mathbb{R} : \epsilon \leq P_a \left(\lim_{N \rightarrow \infty} \log p_a(Y | x, (X_i, Y_i)_1^N) \leq q | F, x, (X, Y)_1^\infty \right) \right\} \quad (17)$$

where we used the fact that $Y \perp (X, Y)_1^\infty | F, x$ in Equation (16). For simplicity, we will use $p(\cdot | (X_i, Y_i)_1^\infty)$ to denote $\lim_{N \rightarrow \infty} p(\cdot | (X_i, Y_i)_1^N)$ with similar conventions from other quantities. Now, applying Doob's to $g(f) = P_a(\log p_a(Y | x, (X_i, Y_i)_1^\infty) \leq q | f, x, (X_i, Y_i)_1^\infty)$ we get that almost surely

$$P_a(\log p_a(Y | x, (X_i, Y_i)_1^\infty) \leq q | F, x, (X_i, Y_i)_1^\infty) \quad (18)$$

$$= \lim_{N \rightarrow \infty} \mathbb{E}_{F \sim p(f | \mathcal{D}_n)} [P_a(\log p_a(Y | x, (X_i, Y_i)_1^\infty) \leq q | F, x, (X_i, Y_i)_1^\infty) | (X_i, Y_i)_1^N] \quad (19)$$

$$= \lim_{N \rightarrow \infty} P_a(\log p_a(Y | x, (X_i, Y_i)_1^\infty) \leq q | (X_i, Y_i)_1^N) \quad (20)$$

$$= P_a(\log p_a(Y | x, (X_i, Y_i)_1^\infty) \leq q | (X_i, Y_i)_1^\infty) \quad (21)$$

where we used Doob's on Equation (19) and the tower property in Equation (20). Plugging this back in Equation (17) we obtain

$$Q_{a,\epsilon}(F, x) = \inf \{ q \in \mathbb{R} : \epsilon \leq P_a(\log p_a(Y | x, (X_i, Y_i)_1^\infty) \leq q | (X_i, Y_i)_1^\infty) \} \quad (22)$$

$$= Q_{a,\epsilon}((X_i, Y_i)_1^\infty, x) \quad (23)$$

To complete the proof, note that

$$\iint \mathbb{1} \{ \log p(y | x, f) < Q_\epsilon(f, x) \} dP(f | \mathcal{D}_n) dP(y | x, \mathcal{D}_n) \quad (24)$$

$$= \iint \mathbb{1} \{ \log p_a(y | x, f) < Q_{a,\epsilon}(f, x) \} dP_a(f) dP(y | x, \mathcal{D}_n) \quad (25)$$

where we changed the probability spaces from p to p_a . This is justified because $p_a(y | x, f) = p(y | x, f, \mathcal{D}_n) = p(y | x, f)$ where we used the independence of Y on \mathcal{D}_n once f is known, the fact that $p_a(f) = p(f | \mathcal{D}_n)$ by definition, and the fact that for the quantile function $Q_{a,\epsilon}(f, x) = Q_\epsilon(f, x)$ because

$$P_a(\log p_a(Y | x, F) \leq q | F, x) = P(\log p(Y | x, F) \leq q | F, x) \quad (26)$$

due again to the independence of Y on the dataset \mathcal{D}_n once f is known. Finally we have (abusing notation using $\mathcal{D}_{n+1}^\infty = (x, y)_{n+1}^\infty$ to refer to $(x, y)_{n+1}^\infty$ in the original probability space but also

$(x_i, y_i)_1^\infty$ in the alternative probability space as they have the same distribution):

$$h_\epsilon(x) = \iint \mathbb{1}\{\log p_a(y | x, f) < Q_{a,\epsilon}(f, x)\} dP_a(f) dP(y | x, \mathcal{D}_n) \quad (27)$$

$$= \iint \mathbb{1}\{\log p_a(y | x, f) < Q_{a,\epsilon}(f, x)\} dP_a(f, (x, y)_{n+1}^\infty) dP(y | x, \mathcal{D}_n) \quad (28)$$

$$= \iint \mathbb{1}\{\log p_a(y | x, \mathcal{D}_{n+1}^\infty) < Q_{a,\epsilon}(\mathcal{D}_{n+1}^\infty, x)\} dP_a(y | x) dP_a(f, \mathcal{D}_{n+1}^\infty) \quad (29)$$

$$= \iint \mathbb{1}\{\log p_a(y | x, \mathcal{D}_{n+1}^\infty) < Q_{a,\epsilon}(\mathcal{D}_{n+1}^\infty, x)\} dP(y | \mathcal{D}_n, x) dP(f, \mathcal{D}_{n+1}^\infty | \mathcal{D}_n) \quad (30)$$

$$= \iint \mathbb{1}\{\log p_a(y | x, \mathcal{D}_{n+1}^\infty) < Q_{a,\epsilon}(\mathcal{D}_{n+1}^\infty, x)\} dP(y | \mathcal{D}_n, x) dP(\mathcal{D}_{n+1}^\infty | \mathcal{D}_n) \quad (31)$$

Where Equation (28) is justified by because $(x, y)_{n+1}^\infty$ doesn't appear in the term inside, Equation (29) is justified by the arguments above and Lemma C.1, and Equation (31) is a result of marginalizing f out. The last thing to point out is that $p_a(y | x, (x, y)_{n+1}^\infty) = p(y | x, (x_i, y_i)_1^\infty)$ and

$$Q_{a,\epsilon}((x, y)_{n+1}^\infty, x) = Q_\epsilon((x_i, y_i)_1^\infty, x)$$

because

$$\begin{aligned} P_a(\log p_a(Y | x, (x, y)_{n+1}^\infty) \leq q | x, (x, y)_{n+1}^\infty) \\ = P(\log p(Y | x, (x_i, y_i)_1^\infty) \leq q | x, (x_i, y_i)_1^\infty) \end{aligned}$$

Using this fact in Equation (31) yields the theorem. \square

D Mutual Information

In the main paper we focus on developing the posterior hallucination rate; however, there are other quantities that can also be used to predict model performance. A common quantity used for this purpose in Bayesian machine learning is the posterior mutual information between F and Y , $I(Y; F | x, \mathcal{D}_n)$. This is often said to quantify *epistemic* uncertainty. The reason for this name is that when we quantify the total predictive uncertainty as the entropy of the posterior predictive $H(Y | x, \mathcal{D}_n)$ and the aleatoric uncertainty—the component of the uncertainty that can't be reduced—as the expected entropy of the likelihood $\mathbb{E}_{p(f|x, \mathcal{D}_n)}[H(Y | f)]$, then the difference is the epistemic uncertainty—the component of the uncertainty that can be reduced. By the definition of mutual information we have

$$\underbrace{I(Y; F | x, \mathcal{D}_n)}_{\text{Epistemic uncertainty}} = \underbrace{H(Y | x, \mathcal{D}_n)}_{\text{Predictive uncertainty}} - \underbrace{\mathbb{E}_{p(f|x, \mathcal{D}_n)}[H(Y | f)]}_{\text{Aleatoric uncertainty}}$$

D.1 Aleatoric Uncertainty

We can define *epistemic uncertainty* by $I(Y; F | x, \mathcal{D}_n)$ which quantifies the expected information we could gain about the mechanism f upon observing a response y conditional on the prompt $((x_i, y_i)_1^n, x)$. Mutual information can be conveniently expressed as a difference in entropies,

$$\begin{aligned} I(Y; F | x, \mathcal{D}_n) &= H(Y | x, \mathcal{D}_n) - \mathbb{E}_{p(f|x, \mathcal{D}_n)}[H(Y | f)] \\ &= -\int \log p(y | x, \mathcal{D}_n) dP(y | x, \mathcal{D}_n) + \iint \log p(y | x, f) dP(y | x, f) dP(f | \mathcal{D}_n). \end{aligned}$$

The first r.h.s. term corresponds to the *predictive entropy* and the second r.h.s. term corresponds to the *aleatoric entropy*. We see that the predictive entropy depends only on the predictive distribution, $p(y | x, \mathcal{D}_n)$, which under our assumptions, is the estimand of a CGM, $p_\theta(y | x, (x_i, y_i)_1^n)$. The aleatoric entropy, on the other hand, depends both on the likelihood function, $p(y | x, f)$, and the posterior over mechanisms, $p(f | x, (x_i, y_i)_1^n)$, which are only latently modeled by a CGM.

In the next section we show how the aleatoric entropy can be expressed using samples from $p(x, y | (x_i, y_i)_1^n)$, which enables its estimation with a CGM and in turn provides a practical estimator for the *epistemic uncertainty* of the model.

D.2 Aleatoric Entropy for Conditional Generative Models

Theorem 4. Assume that the conditions of Theorem 1 hold for F and (X, Y) . Then,

$$\mathbb{E}_{p(f|x, \mathcal{D}_n)} [H(Y | f)] = \mathbb{E}_{p(\mathcal{D}_{n+1}^\infty | x, \mathcal{D}_n)} [H(Y | x, \mathcal{D}_\infty)].$$

Note the abuse of notation where the element $x_{n+1} \in \mathcal{D}_{n+1}^\infty := (x_i, y_i)_{n+1}^{\inf}$ will be taken as the query x .

Proof.

$$\begin{aligned} \mathbb{E}_{p(f|x, \mathcal{D}_n)} [H(Y | f, x)] &= \int H(Y | f, x, \mathcal{D}_n) dP(f | x, \mathcal{D}_n) \\ &= \iint -\log p(y | f, x, \mathcal{D}_n) dP(y | f, x, \mathcal{D}_n) dP(f | x, \mathcal{D}_n) \\ &= \iint -\log p_a(y | f) dP_a(y | f) dP_a(f) \\ &= \int -\log p_a(y | f) dP_a(y, f) \\ &= \int -\log p_a(y | f) dP_a(y, f, \mathcal{D}_{n+1}^\infty) \\ &= \int -\log p_a(y | \mathcal{D}_{n+1}^\infty) dP_a(y, f, \mathcal{D}_{n+1}^\infty) && \text{Lemma C.1} \\ &= \int -\log p_a(y | \mathcal{D}_{n+1}^\infty) dP_a(y, \mathcal{D}_{n+1}^\infty) \\ &= \iint -\log p_a(y | \mathcal{D}_{n+1}^\infty) dP_a(y | \mathcal{D}_{n+1}^\infty) dP_a(\mathcal{D}_{n+1}^\infty) \\ &= \iint -\log p(y | x, \mathcal{D}_\infty) dP(y | x, \mathcal{D}_\infty) dP(\mathcal{D}_{n+1}^\infty | x, \mathcal{D}_n) \\ &= \mathbb{E}_{p(\mathcal{D}_{n+1}^\infty | x, \mathcal{D}_n)} [H(Y | \mathcal{D}_\infty, x)] \end{aligned}$$

□

D.3 Estimators

Inspired by the methodology in the paper, we follow a similar process for obtaining approximate estimates of the aleatoric uncertainty and epistemic uncertainties.

In particular we let,

$$H_\theta(Y | F, (x_i, y_i)_1^n, x) := - \int g_\theta^H((x_i, y_i)_1^N, x) dP_\theta(x^{n+1:N} | (x_i, y_i)_1^n),$$

where

$$g_\theta^H((x_i, y_i)_1^N, x) := \int \log p_\theta(y | (x_i, y_i)_1^N, x) dP_\theta(y | (x_i, y_i)_1^N, x), \quad (33)$$

and $N - n$ is a practical number of generated examples. This model approximation for the aleatoric entropy allows us to define a model approximation for the mutual information.

$$I_\theta(Y; F | (x_i, y_i)_1^n, x) := H_\theta(Y | (x_i, y_i)_1^n, x) - H_\theta(Y | F, (x_i, y_i)_1^n, x). \quad (34)$$

In turn, we can construct practical Monte-Carlo estimators for $H_\theta(Y | (x_i, y_i)_1^n, x)$, $g_\theta^H((x_i, y_i)_1^N, x)$, and $H_\theta(Y | F, (x_i, y_i)_1^n, x)$ using predictive resampling [39]. These estimators are described below and the predictive resampling algorithm is described in Algorithm 3.

Predictive entropy.

$$\hat{H}_\theta(Y | (x_i, y_i)_1^n, x) := -\frac{1}{M} \sum_{i=1}^M \log p_\theta(y_i | (x_i, y_i)_1^n, x), \quad y_i \sim p_\theta(y | (x_i, y_i)_1^n, x) \quad (35)$$

Aleatoric entropy.

$$\hat{g}_{\theta}^H((x_i, y_i)_1^N, x) := -\frac{1}{M} \sum_{i=1}^M \log p_{\theta}(y_i | (x_i, y_i)_1^N, x), \quad y_i \sim p_{\theta}(y | (x_i, y_i)_1^N, x) \quad (36)$$

$$\hat{H}_{\theta}(Y | F, (x_i, y_i)_1^n, x) := \text{PredictiveResampling}(x, (x_i, y_i)_1^n, \hat{g}_{\theta}^H((x_i, y_i)_1^N, x)) \quad (37)$$

Mutual information

$$\hat{I}_{\theta}(Y; F | (x_i, y_i)_1^n, x) := \hat{H}_{\theta}(Y | (x_i, y_i)_1^n, x) - \hat{H}_{\theta}(Y | F, (x_i, y_i)_1^n, x) \quad (38)$$

Algorithm 3 PredictiveResampling($x, (x_i, y_i)_1^n, \hat{g}_{\theta}((x_i, y_i)_1^N, x)$)

Require: query x , context $(x_i, y_i)_1^n$, functional $\hat{g}_{\theta}((x_i, y_i)_1^N, x)$, # MC samples M , max context length N .

- 1: **for** $i \leftarrow 1$ to M **do**
 - 2: $(x_i, y_i)_1^N \leftarrow (x_i, y_i)_1^n$ ▷ initialize context
 - 3: **for** $j \leftarrow n + 1$ to N **do**
 - 4: $(x_j, y_j) \sim p_{\theta}(x, y | (x_i, y_i)_1^N)$ ▷ sample example from model
 - 5: $(x_i, y_i)_1^N \leftarrow ((x_i, y_i)_1^N, x_j, y_j)$ ▷ update context
 - 6: $g_{i,N} \leftarrow \hat{g}_{\theta}((x_i, y_i)_1^N, x)$ ▷ evaluate functional
 - 7: **return** $\frac{1}{M} \sum_{i=1}^M g_{i,N}$ ▷ estimate expectation
-

E Evaluation Details

E.1 Synthetic

We implement our neural process by modifying the Llama 2 architecture [42] to model sequences of continuous variables. We replace the tokenizer by a linear layer and the output categorical distribution by a Riemann distribution [7]. We train the model from random initialization on sequences of (x, y) pairs using a standard next token prediction objective and use the AdamW optimizer [82] with `learning_rate` = 0.0001, $\beta_1 = 0.9$, $\beta_2 = 0.999$, $\epsilon = 1e-8$, and `weight_decay` = $1e-6$ ³. We use a cosine learning rate schedule, with warmup of 2000 steps, and decay final learning rate down to 10% of the peak learning rate.

We define the $(1-\epsilon)$ -likely set with $\epsilon = 0.05$ such that a response y is a hallucination if it falls outside of the 95% confidence interval of a given sampled distribution conditioned on x . The data generating process is described in Appendix F.1.

E.2 Language

We consider tasks defined by six datasets: **Stanford Sentiment Treebank (SST2)** [49]: predict sentiment *positive* or *negative*; **Subjectivity** [50]: predict review *subjective* or *objective*; **AG News** [6]: predict article *World*, *Sports*, *Business* or *Sci/Tech*; **Medical QP** [51]: predict medical question pairs as *similar* or *dissimilar*; **RTE** [52]: predict two sentences as *entailment* or *not entailment*; and **WNLI** [53]: predict sentence with pronoun replaced as *entailment* or *not entailment*. We replace the label *Sci/Tech* with *Science* for AG News and *not entailment* by *not* for RTE and WNLI. We filter out any queries of length longer than 116 tokens. Full descriptions of these datasets are given in Appendix F.2.

To implement ICL for a given dataset, we sample a response balanced training set of query/response pairs $\mathcal{D}_{\text{train}} = (x_i, y_i)_1^n$. Each query in $\mathcal{D}_{\text{train}}$ is prepended with the string `Input:` and appended with a new line `.` Each response is prepended with the `Label:` and appended with `\n\n`. A test query x_{test} is prepended with the `Input:` and appended with `\nLabel: .` These strings are concatenated

³ This process is similar to the “prior fitted network” implementation of Müller et al. [7], but we require the conditional distribution of both queries x and responses y , where their implementation only models responses.

together to form a prompt and we generate a response y from the predictive distribution given by a Llama-2 model $p_{\theta}(y \mid \mathcal{D}_{\text{train}}, x_{\text{test}})$. An example prompt from the Subjectivity dataset is shown in Appendix E.2.

For our experiments in 3.2, we employ LLaMA-2 [42], a family of open source LLMs based on an auto-regressive transformer, pretrained on 2 trillion tokens with a context window of 4,096 tokens. We run LLaMA-2-7B as an unquantized model (16-bit).

To estimate the predictive distribution over responses, we sample n input/label pairs based on the given context length, create a prompt based on the context, and generate a number of y samples. An example of a prompt from the Subj dataset is set forth in Figure 7.

```

Input: the assassins force walter to drive their escape car .
Label: objective

Input: vega and ulloa give strong performances as the leading
      lovers and there are some strong supporting turns ,
      particularly from najwa nimri .
Label: subjective

Input: they decide that the path to true love is to purposely
      set each other up on ‘‘ extreme dates ‘‘ with the
      objects of their affections .
Label: objective

Input: ‘‘ maid in manhattan ‘‘ is a charmer , a pc ‘‘ pretty
      woman ‘‘ that ditches the odious prostitution theme for
      class commentary
Label: subjective

Input: each weekend they come back with nothing but a hangover
Label: objective

Input: piccoli ’s performance is amazing , yes , but the
      symbols of loss and denial and life-at-arm’s-length in
      the film seem irritatingly transparent .
Label:

```

Figure 7: Example prompt for language model

The y samples are generated as single tokens, since all labels for our datasets can be identified based on their first token. We set the `temperature` and `top_p` parameters to 1 to provide the greatest possible diversity and randomness to the label output.

For predictive sampling, we initialize the context by sampling n input/label pairs, generate $N - n$ new context examples by producing prompts that include the updated context, and produce a number of y samples from the cumulative context. For the generated context examples, we set `max_new_tokens` = 200, `temperature` = 1 and `top_p` = 0.9 to provide a high level diversity and randomness to the generated output. Examples of generated context pairs are set forth in Figure 8.

Using the transition scores from the model outputs, we compute the log likelihood needed for the posterior hallucination rate.

F Dataset Details

F.1 Synthetic

Queries x are sampled from a uniform distribution on $[-2, 2]$. Responses y are sampled from a normal distribution with mean $\mu(x)$ parameterized by a random ReLU neural network conditioned on x and constant standard deviation $\sigma = 0.1$. We generate a set of 8000 sequences, each corresponding to a distinct random re-initialization of the neural network, with 2000 (x, y) examples each. Training and

Input: pick any word , even the tiniest , and you will find
 writers arguing over its relative importance , its
 ' correct ' usage and how you pronounce it .
 Label: objective
 Input: janus' entry does a number of things the novel fails at
 : it tells the story of the novel and , better yet ,
 it 's funny .
 Label: subjective
 Input: this is the kind of show that 's got the warm n'
 fuzzies all over , especially if you have a sick sense
 of humor .
 Label: subjective
 Input: even if you are an apple and orange man or woman who
 would be more comfortable at a state fair rodeo than
 in a silk dress , this should be on your list .
 Label: objective
 Input: nearly every adjective one could use to describe a
 movie theater , except expensive and first-run , can
 be used to describe this place .
 Label: subjective

Figure 8: Example of generated context pairs

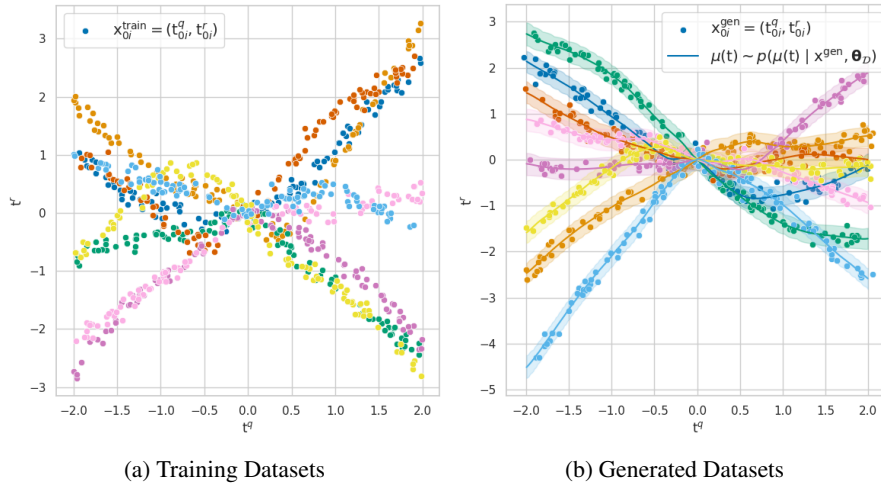


Figure 9: Training and generated datasets for the synthetic regression task.

test data are generated over non-overlapping sets of generated sequences. Example training datasets are plotted as different colors in Figure 9.

F.2 Language

For our experiments in 3.2, we randomly sample context examples and test input/label pairs from the following datasets:

Stanford Sentiment Treebank (SST2) SST2 [49] is a corpus with fully labeled parse trees that allows for a complete analysis of the compositional effects of sentiment in language. The corpus consists of 11,855 single sentences extracted from movie reviews. It was parsed with the Stanford parser and includes a total of 215,154 unique phrases from those parse trees, each annotated by 3 human judges. Sentiments are classified as binary labels "positive" or "negative".

Subjectivity (Subj) The subjectivity dataset [50] contains 5,000 movie review snippets from www.rottentomatoes.com labeled "subjective", and 5,000 sentences from plot summaries available

from www.imdb.com labeled "objective". Selected sentences or snippets are at least ten words long and are drawn from movies released post-2001.

AG News The AG News dataset [6] contains 496,835 categorized news articles from more than 2,000 news sources. The 4 largest classes (World, Sports, Business, Sci/Tech) were chosen from this corpus to construct our dataset, including only the title and description fields.

Medical Questions Pairs (MQP) The MQP dataset [51] consists of 3,048 similar and dissimilar medical question pairs hand-generated and labeled by doctors based on patient-asked questions randomly sampled from HealthTap. Each question results in one positive question pair ("similar") that looks very different by superficial metrics, and a negative question pair ("different") that conversely look very similar, so as to ensure that the task is not trivial.

Recognizing Textual Entailment (RTE) The RTE dataset [52] comes from a series of annual textual entailment challenges. Examples are constructed based on news and Wikipedia text, and labeled as binary classifications based on whether or not there is entailment.

Winograd Schema Challenge (WNLI) The WNLI dataset [53] consists of 1,100 sentence pairs with ambiguous pronouns with different possible referents. The task is to predict if the sentence with the pronoun substituted is entailed by the original sentence.

G Additional Results

G.1 Synthetic

We extend the synthetic experiments in the paper in two ways. First, we provide additional results for the setup described in the main sections. Second, we provide additional results in a controlled experiment where we have access to analytic expressions for the posterior predictive.

G.1.1 Additional results with main paper setup

Figure 10 displays scatter plots of the true hallucination rate against the posterior hallucination rate over various context lengths (number of in-context examples) and values of the ϵ parameter. We can see that the trends reported Section 3.1 hold across different values for ϵ .

Figure 11 adds additional evidence for our reported findings and demonstrates performance over different ϵ settings.

Figure 12 shows scatter plots of the true probability of hallucination vs. the PHR under misspecified ϵ values. The THR is calculated under $\epsilon = 0.05$. From top to bottom we show charts for different epsilon values, denoted as $\tilde{\epsilon}$, used to calculate the PHR. Notably, when we compare $\tilde{\epsilon} = 0.1$ to $\tilde{\epsilon} = 0.05$, we see that for the PHR is a more accurate predictor of the THR when the PHR is calculated with a higher ϵ value. This reflects our observation that the PHR underestimates the THR, particularly for longer context lengths (more in-context examples n).

Mutual information. We also evaluate the mutual information (MI) estimator (Equation (38)) as a predictor of the true hallucination rate (THR). Appendix G.1.1 shows that the MI estimates are significantly correlated with the THR, which indicates that the MI can also be an effective predictor of hallucinations. Figure 14 allows us to look deeper into the relationships between the THR, PHR, and MI. In comparing Figures 14a and 14b, we see that the PHR has a more linear relationship to the THR than the MI, which has a more sigmoidal relationship to the THR. This sigmoidal relationship is amplified when plotting the PHR against the MI in Figure 14c. This provides evidence that the PHR and MI encode the same type of information, and that the PHR is a measure of epistemic uncertainty.

G.2 Language

G.2.1 Gemma-2

Here we evaluate the posterior hallucination rate estimator on common natural language in-context learning tasks using Gemma-2 9B [43].

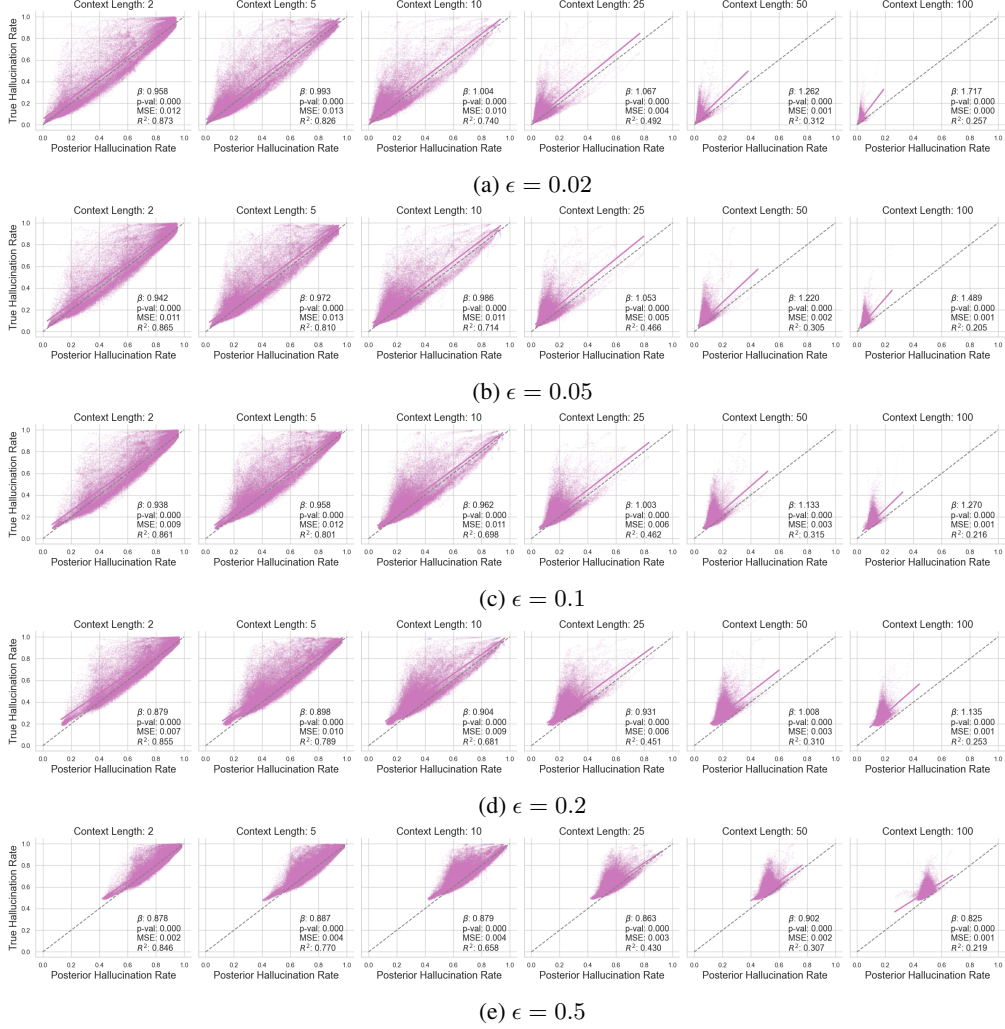


Figure 10: Synthetic regression data ablation of the ϵ parameter. Scatter plots of the true hallucination rate against the posterior hallucination rate. We observe that the posterior hallucination rate is an accurate predictor of the true hallucination rate under various settings of the ϵ parameter value.

Figure 15 shows the error rate (top) and response entropy (bottom) of Gemma-2-9b. In general, both metrics decrease and saturate with longer context lengths. For all tasks, the model performs better than random, indicating it may generalize to these tasks ("in-capability"). For Medical QP and WNLI, error rates begin to decrease, but then get closer to random, indicating poor generalization ("out-of-capability"). The posterior hallucination rate estimator is designed for in-capability tasks and is ill-defined for out-of-capability tasks.

Results. We report results for Gemma-2-9b. We set $N - n = 5$, $M = 10$, and $K = 50$. Figure 16 plots the MHR and estimated posterior hallucination rate against the number of in-context examples with $\epsilon = 0.05$. It shows that the posterior hallucination rate is a good estimator of the MHR. We show that this trend holds for Llama-2 models and alternative settings of ϵ in Figures 4a and 18 of Appendix G.2.2.

Figure 17 plots the empirical error rate and estimated posterior hallucination rate against the number of in-context examples with $\epsilon = 0.75$. For the in-capability tasks (SST2, Subjective, AG News, and RTE), it shows that the posterior hallucination rate accurately tracks the error rate when ϵ is set to a high value. For the out-of-capability tasks (Medical QP, and WNLI), we observe that this is not the case as expected.

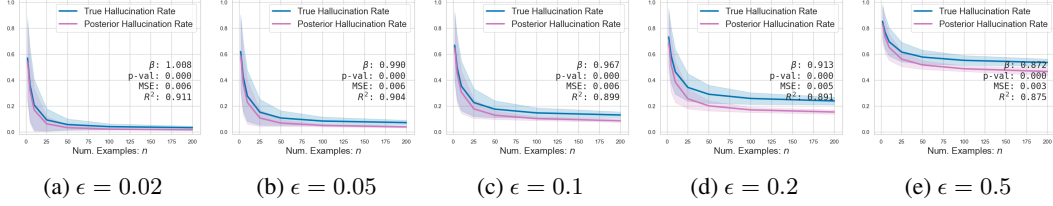


Figure 11: Synthetic regression data ablation of the ϵ parameter. Plotting the true and posterior hallucination rates (THR and PHR) against the number of in-context examples n . We observe that the PHR is a good predictor of the THR across different settings of ϵ . Further, we observe that the PHR is a more accurate estimator for small ϵ values than for large ϵ values.

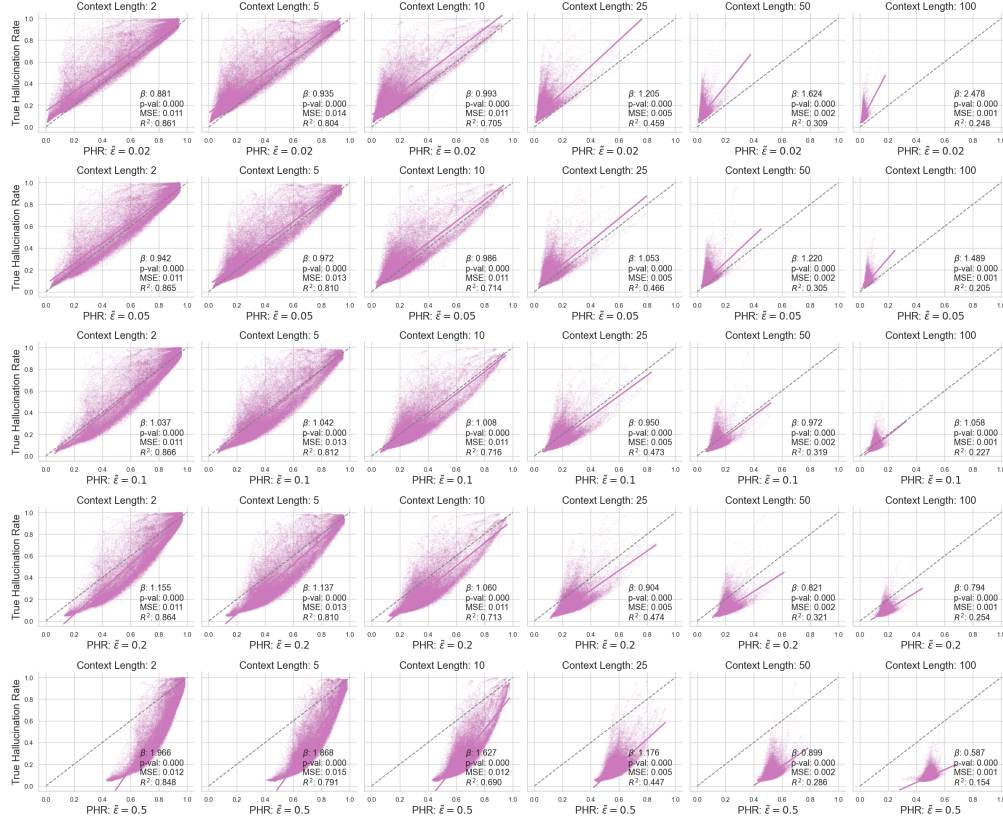


Figure 12: **Synthetic data:** Effect of misspecified ϵ . The true value is $\epsilon = 0.05$ and is used to calculate the THR. We vary the value used in calculating the posterior hallucination rate, which we denote as $\tilde{\epsilon}$ here.

G.2.2 Llama-2

Here we evaluate the posterior hallucination rate estimator on common natural language in-context learning tasks using the Llama-2 family of LLMs [42]. Descriptions of all data sets and pre-processing are given in Appendix F.2.

To implement ICL for a given dataset, we sample a response balanced training set of query/response pairs $\mathcal{D}_n = (\mathbf{x}_i, \mathbf{y}_i)_{i=1}^n$. We generate a response \mathbf{y} from the predictive distribution given by a Llama-2 model $p_{\theta}(\mathbf{y} \mid \mathcal{D}_n, \mathbf{x})$. We structure the prompt by adding strings to distinguish between inputs and labels. An example prompt from the Subjectivity dataset is shown in Appendix E.2.

Figure 5 shows the error rate (top) and response entropy (bottom) of Llama-2-7b. Both metrics decrease and saturate with longer context lengths. For SST2, Subjective, and AG News, the model performs better than random, indicating it can generalize to these tasks ("in-capability"). For

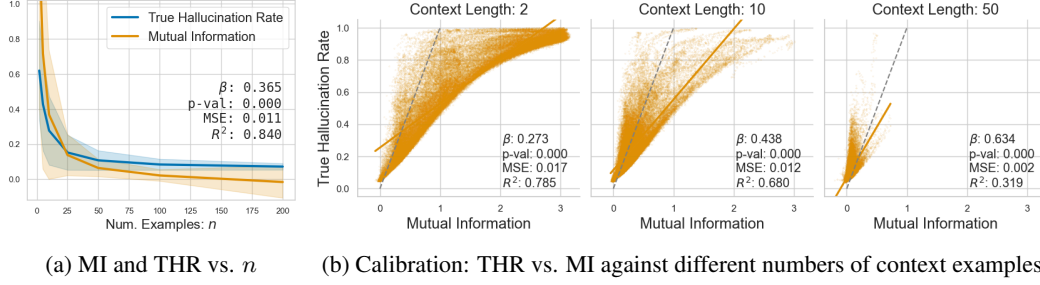


Figure 13: **Synthetic data:** (a) The THR and Mutual Information reduce significantly as the number of contextual examples n increases. (b) Calibration evaluation of the mutual information against the true probability of hallucination given $\epsilon = 0.05$.

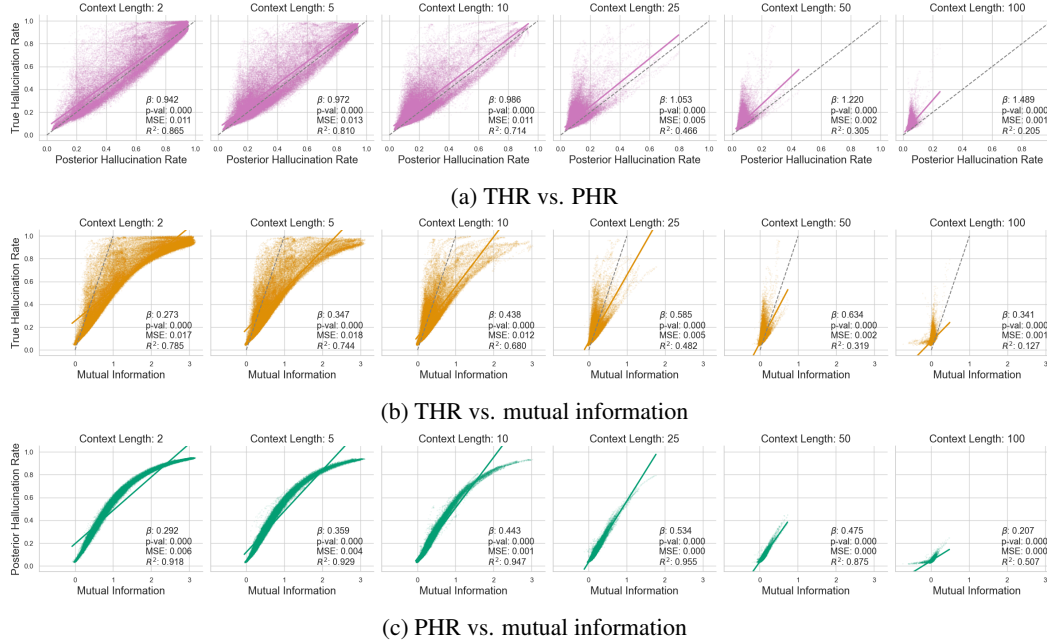


Figure 14: **Synthetic data:** visualizing and quantifying the relationship between the posterior hallucination rate and mutual information.

Medical QP, RTE, and WNLI, error rates are close to random, indicating poor generalization ("out-of-capability"). The posterior hallucination rate estimator is designed for in-capability tasks and is ill-defined for out-of-capability tasks.

Results. We report results for Llama-2-7b. We set $N - n = 5$, $M = 10$, and $K = 50$. Figure 4a plots the MHR and estimated posterior hallucination rate against the number of in-context examples

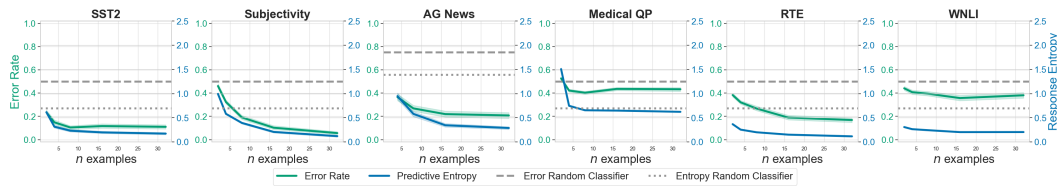


Figure 15: **Gemma-2-9b:** Error Rate (green curves) and Response Entropy (blue curves) on LLM in-context learning tasks. Grey dashed lines represent the error rate and entropy of a random classifier over the set of valid responses.

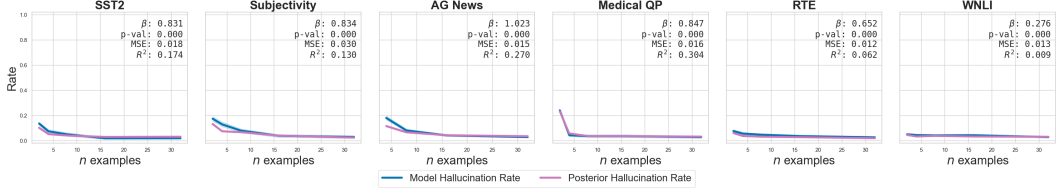


Figure 16: MHR and PHR against number of in-context examples for Gemma-2-9b. We set $\epsilon = 0.05$, and the Posterior Hallucination Rate accurately tracks the Model Hallucination Probability for all tasks (SST2, Subjective, AG News, Medical QP, RTE, and WNLI).

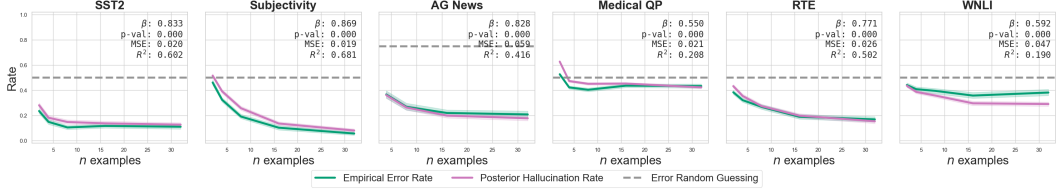


Figure 17: Error rate and PHR against number of in-context examples for Gemma-2-9b. When we set ϵ high (e.g., >0.5), we see that the PHR accurately tracks the Empirical Error Rate for all datasets except for WNLI. The Posterior Hallucination Rate is a considerably worse estimator as this tasks is out-of-capability for Gemma-2-9b.

with $\epsilon = 0.05$. It shows that the posterior hallucination rate is a good estimator of the MHR. We show that this trend holds for alternative settings of ϵ in Figure 18 of Appendix G.

Figure 4b plots the empirical error rate and estimated posterior hallucination rate against the number of in-context examples with $\epsilon = 0.75$. For the in-capability tasks (SST2, Subjective, and AG News), it shows that the posterior hallucination rate accurately tracks the error rate when ϵ is set to a high value. For the out-of-capability tasks (Medical QP, RTE, and WNLI), we observe that this is not the case as expected. We ablate the ϵ parameter and report results in Figure 19 of Appendix G.

Table 1 reports the results of an ablation study on SST2 that varies the number of generated examples, MC samples, y samples, and model parameters. We see that increasing the number of MC samples and number of y samples shows improvement in the R^2 scores for both MHR and the empirical error rate. Whereas increasing the number of generated samples or model size alone shows a decrease in performance on this task.

Table 1: SST2, Llama-2 ablation of hyper parameters for the posterior hallucination rate estimator

MHR		Error Rate		# Generated	# MC Samples	# y samples	# Params
MAE	R^2	MAE	R^2	$N - n$	M	K	
0.039	0.618	0.041	0.702	5	10	50	7B
0.045	0.611	0.045	0.705	10	10	50	7B
0.039	0.618	0.041	0.702	5	10	50	7B
0.038	0.653	0.041	0.711	5	20	50	7B
0.039	0.618	0.041	0.702	5	10	50	7B
0.032	0.681	0.042	0.710	5	10	100	7B
0.039	0.618	0.041	0.702	5	10	50	7B
0.040	0.652	0.042	0.764	5	20	100	7B
0.037	0.689	0.044	0.719	10	20	100	7B
0.039	0.618	0.041	0.702	5	10	50	7B
0.033	0.607	0.041	0.669	5	10	50	13B
0.035	0.669	0.042	0.729	5	20	100	13B

Mutual Information. In Figure 20 we compare the mutual information (MI) estimator to the error rate, model hallucination rate, and posterior hallucination rate. Figure 20a shows that the MI is significantly correlated with the error rate across tasks. Figure 20b shows that the MI is also significantly correlated with the model hallucination rate across tasks. Finally, Figure 20c shows the relationship between the mutual information and posterior hallucination rate across tasks and context lengths. The high R^2 value is further evidence that both estimators measure the same kind of information.

H Computational Requirements

For our experiments, we used an internal cluster made up of A100s and RTX 8000s, which contained between 40 to 48 GBs of GPU memory. Training the models used for the synthetic experiments took about a day on one machine. For the main paper natural language results, we ran 50 seeds per dataset, where a single experiment seed took anywhere between 20 minutes and 4 hrs. We also ablated over different values of M and N (as shown in Appendix G). We ran additional experiments and developed models which required additional compute that were not included in the paper.

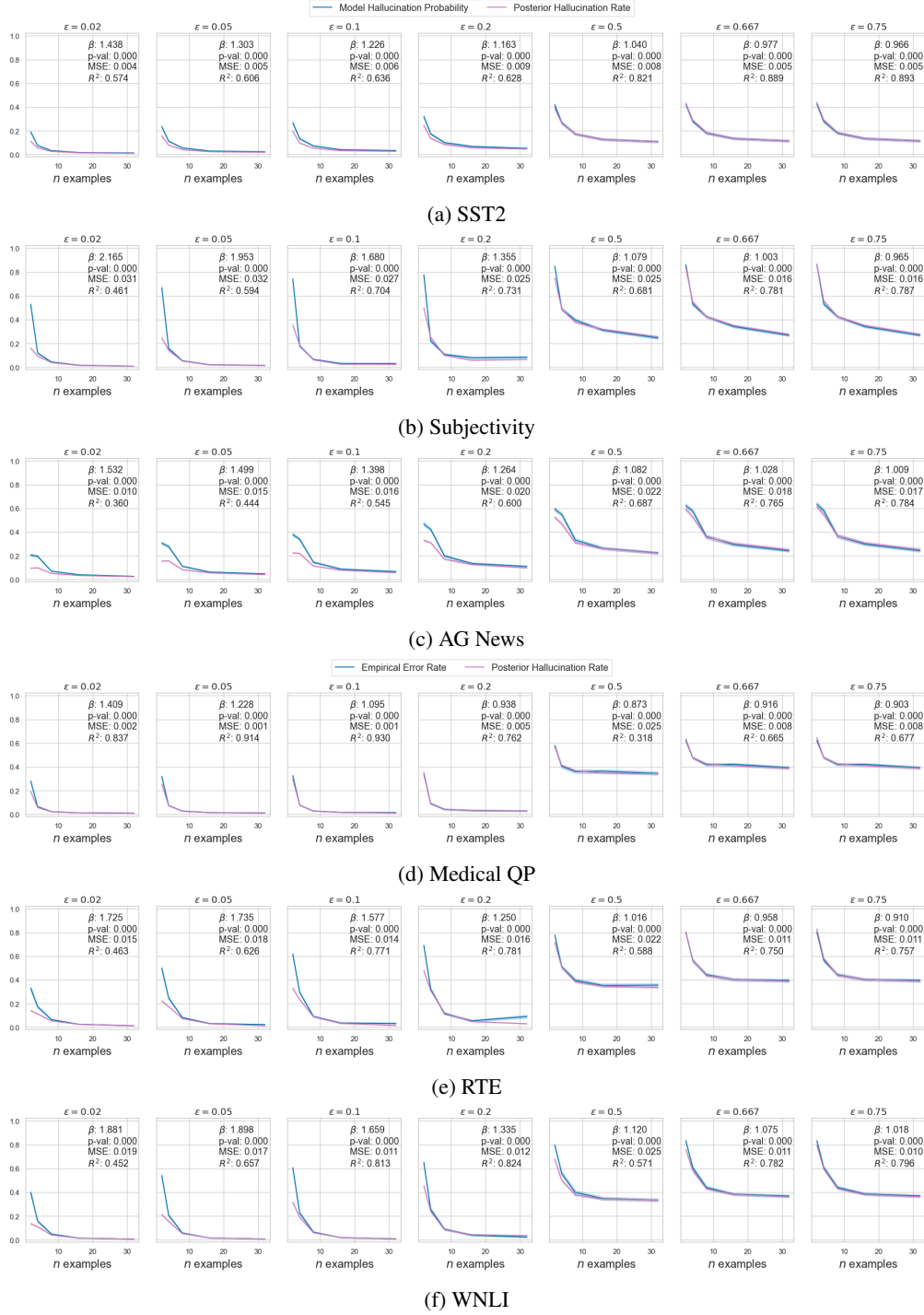


Figure 18: Ablating ϵ for the posterior hallucination rate estimator against the model probability of hallucination for Llama-2-7B.

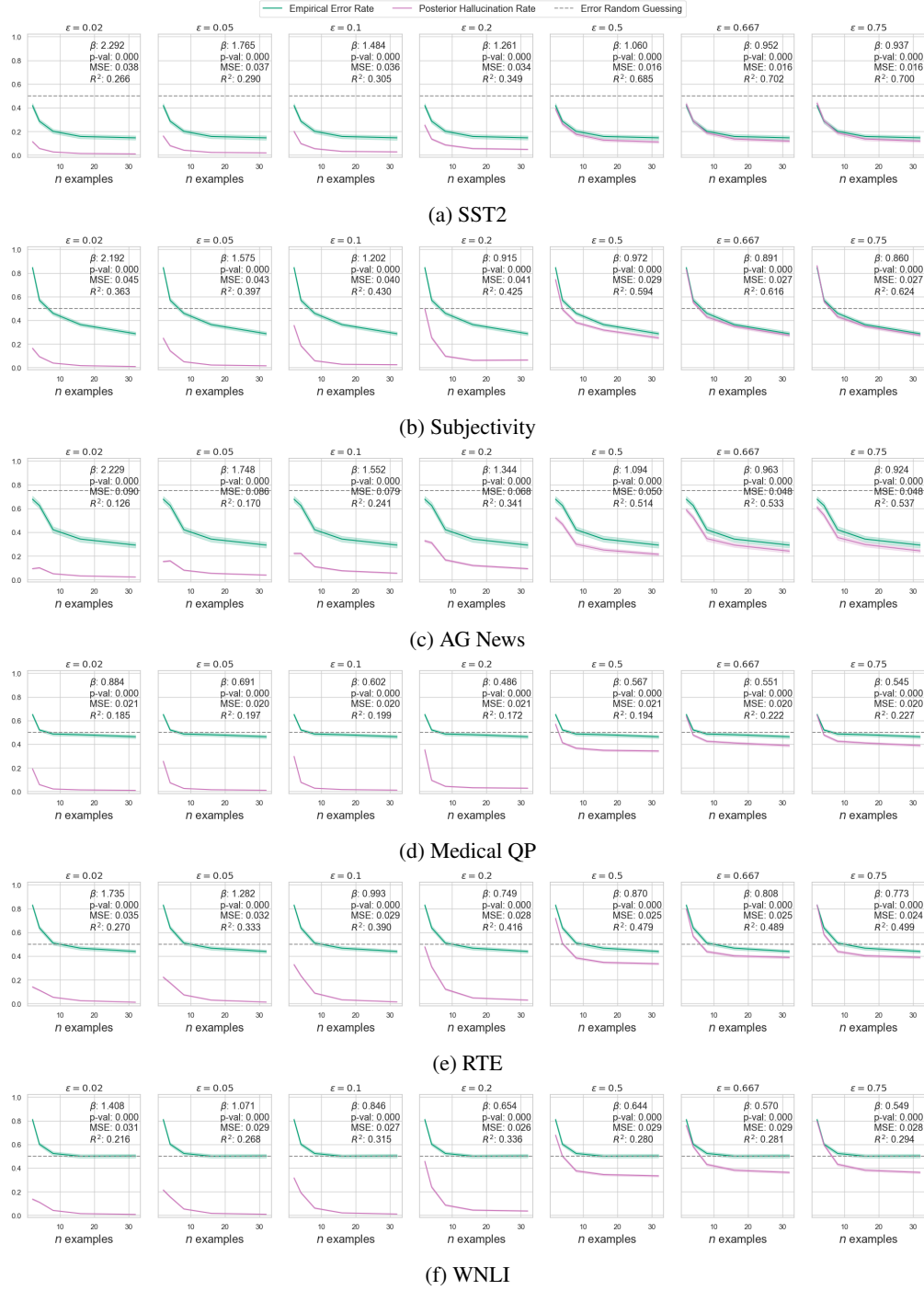
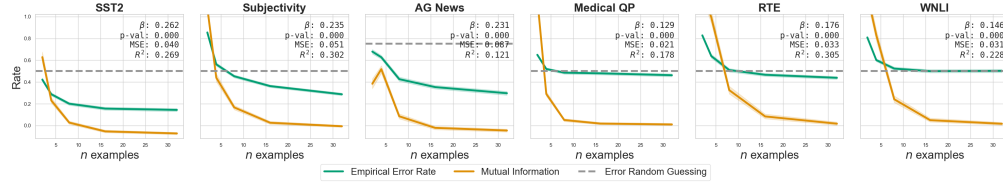
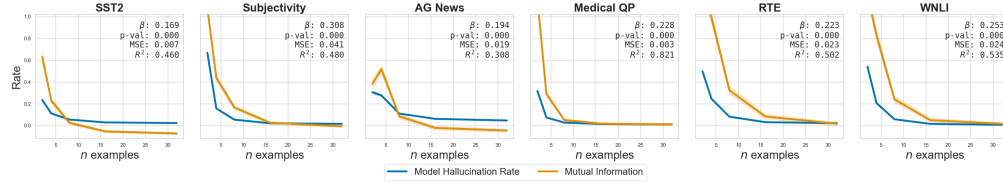


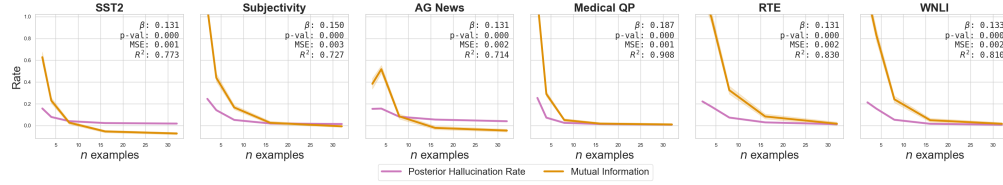
Figure 19: Ablating ϵ for the posterior hallucination rate estimator against the empirical error rate for Llama-2-7B.



(a) Mutual information and error rate vs. n examples.



(b) Mutual information and MHR vs. n examples.



(c) Mutual information and PHR vs. n examples.

Figure 20: Comparing the mutual information estimator to (a) the error rate, (b) the model hallucination rate, and (c) the posterior hallucination rate using Llama-2-7B. We see that there are significant correlations to either metric across tasks. The high R^2 between the mutual information and posterior hallucination rate is evidence that they quantify similar information.